AD-A190 487 ION IMPLANTATION MANUFACTURING TECHNOLOGY PROJECT(U) 1/1
SPIRE CORP BEDFORD MA JAN 87 SPIRE-FR-10089 NRL-574412
N00014-83-C-2221

UNCLASSIFIED F/G 13/8 NL

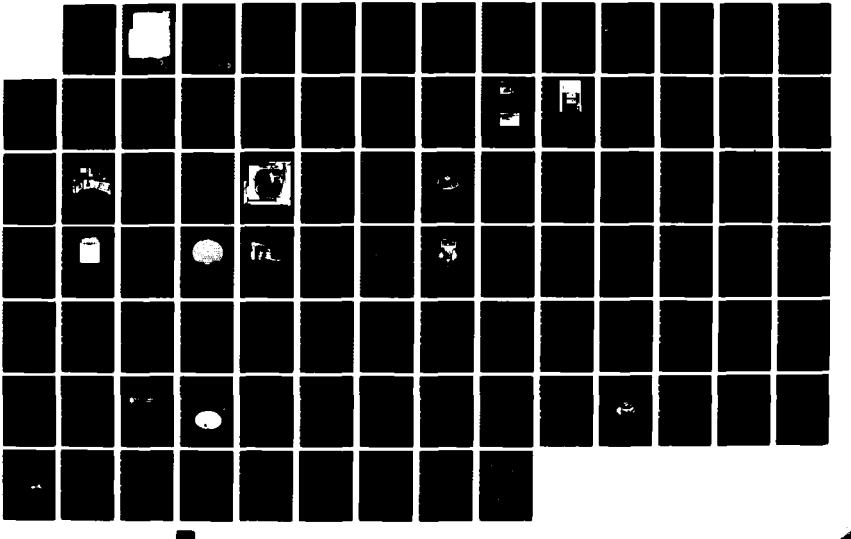

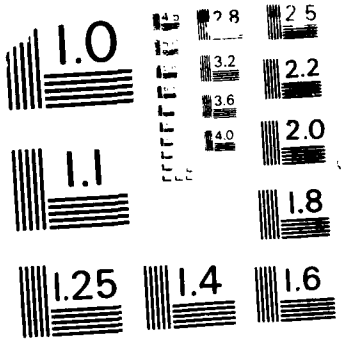

NRL 574432

FR-10089

AD-A190 487

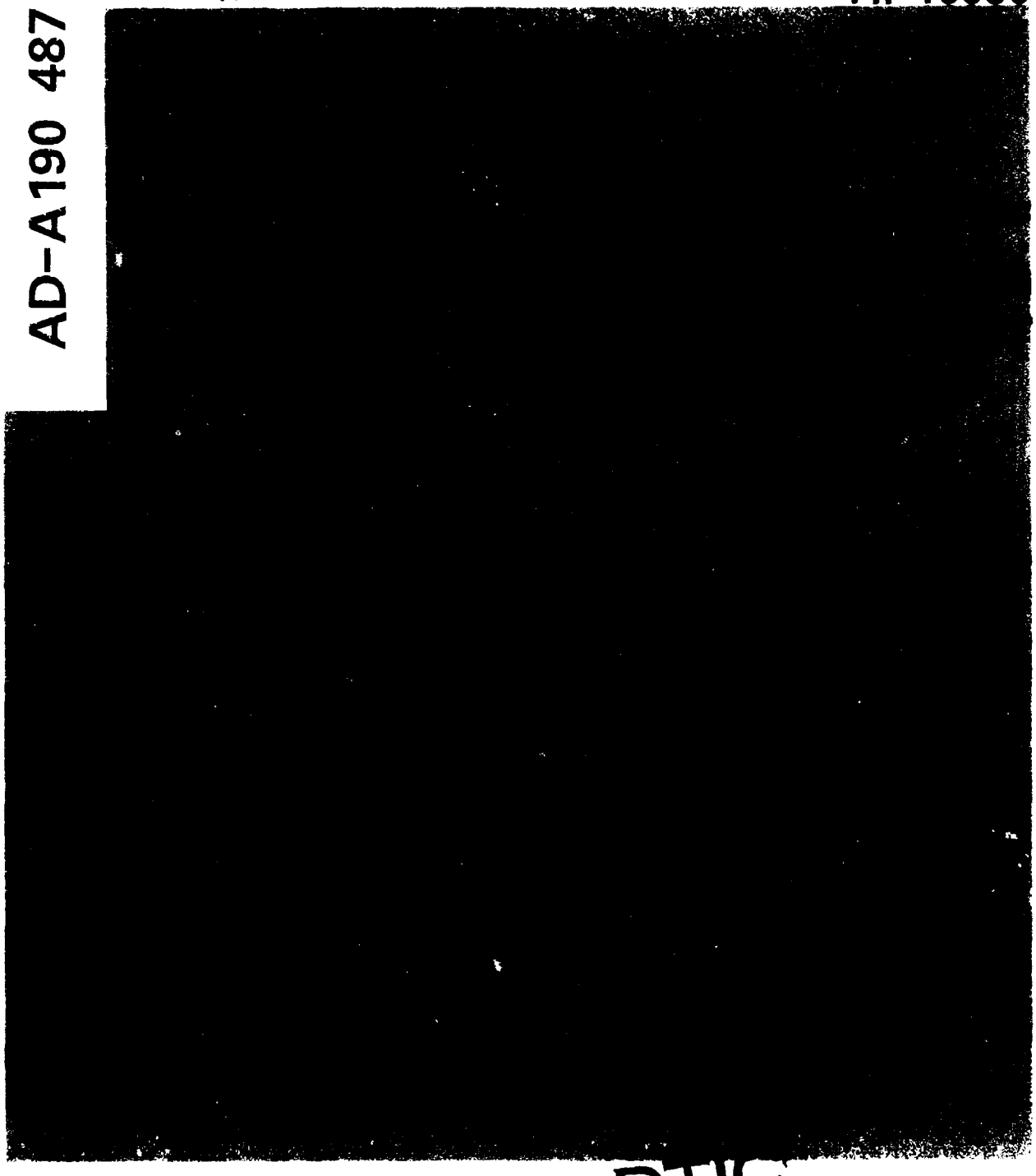

APPROVED FOR PUBLIC RELEASE

DISTRIBUTION UNLIMITED

spire

FR-10089
FR-10097

Final Report for:
ION IMPLANTATION MANUFACTURING TECHNOLOGY PROJECT

January 1987

Contract Numbers: N00014-83-C-2221 and
N00014-85-C-5133

Submitted to:
NAVAL RESEARCH LABORATORY
Washington, DC 20375

Submitted by:
SPIRE CORPORATION
Patriots Park
Bedford, MA 01730

TABLE OF CONTENTS

LIST OF ILLUSTRATIONS

LIST OF ILLUSTRATIONS (Concluded)

LIST OF TABLES

SECTION 1
INTRODUCTION

The objective of the NRL MANTECH Program was to design, build, and operate a high-throughput ion implantation facility. This facility is to be used to demonstrate the transfer of implantation technology to industrial pilot production conditions.

The program consisted of three phases, each intended to involve one year of effort. The first involved design of a vacuum end station with compatible high-throughput workpiece-handling fixtures. Phase 2 consisted of fabrication of this hardware, together with development tests to define implantation conditions for WC tooling. The last phase was to merge a government-funded implanter with the Spire-developed hardware and operate the system as a pilot production facility for the implantation of various Navy bearings for corrosion resistance.

This final report covers all phases of the program, including beam system design, target manipulation, system performance, and cost analyses based on actual/future design concepts.

SECTION 2
SYSTEM DEFINITION

Figure 2-1 shows an overall view of the Navy MANTECH implantation system, consisting of a Government supplied high current ion implanter (Eaton/Nova Model NV-10-160) coupled with a beam transport/target handling system designed and built by Spire Corporation.

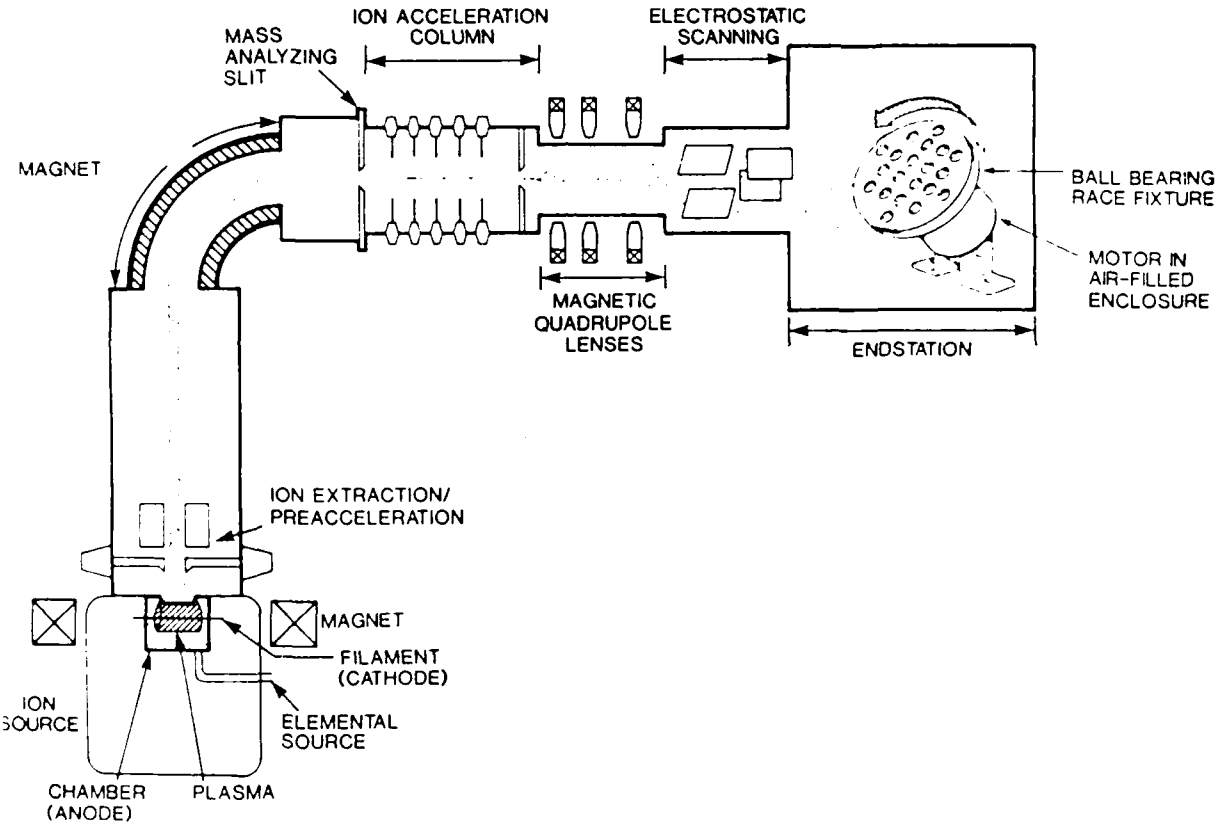

FIGURE 2-1. MANTECH IMPLANTATION SYSTEM.

Figure 2-2 shows an early design concept for the MANTECH implanter end station. The principal components and fixtures have been identified on the figure. The incoming ion beam is from the government furnished equipment (GFE) implanter. Magnetic lenses either i) defocus the beam and create a large spot at the workpiece handling fixture or ii) focus the beam and enable special high voltage scan plates to raster scan the beam to ensure spatial uniformity at the target.

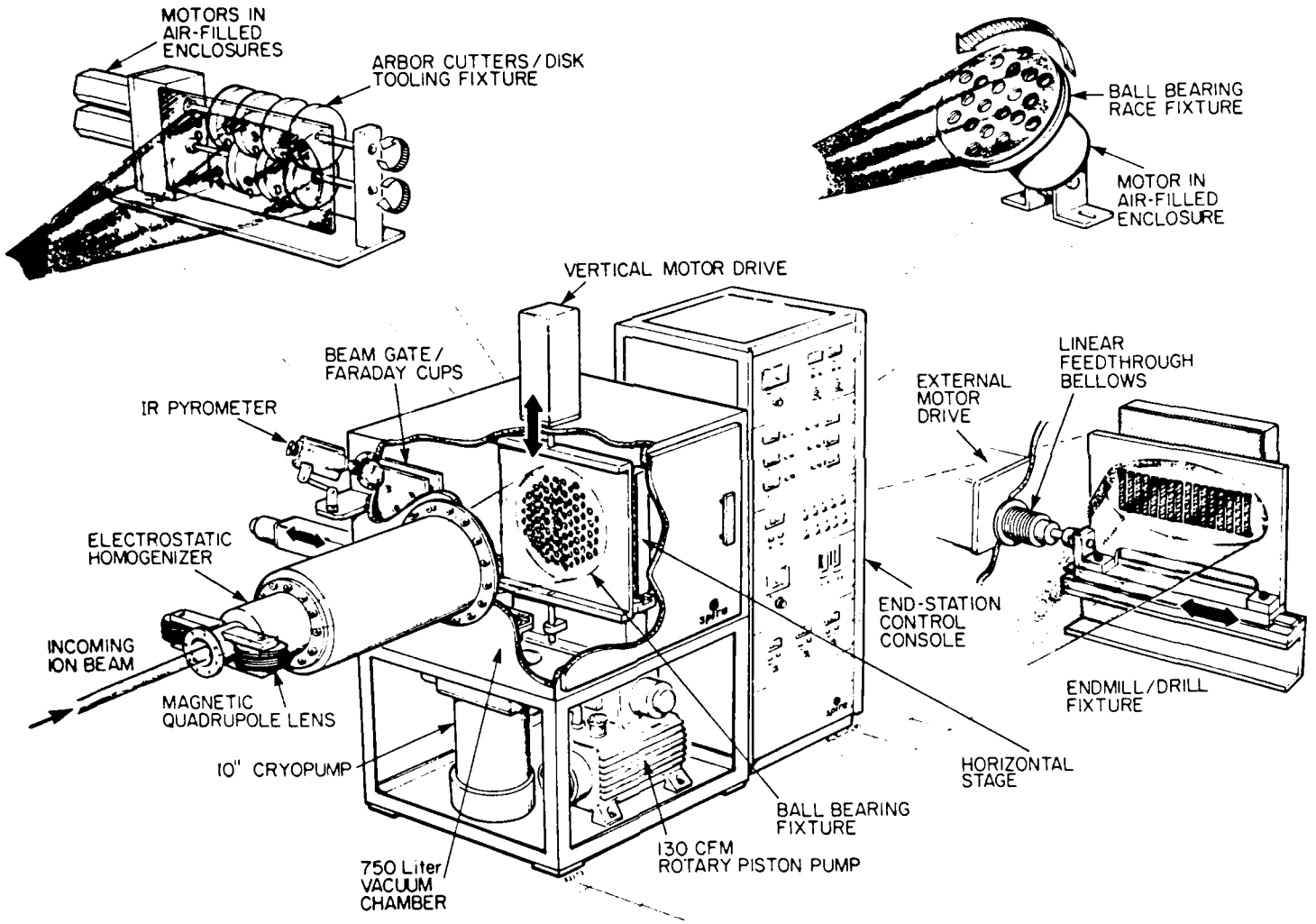

FIGURE 2-2. END STATION SYSTEM.

2.1 IMPLANTATION PROCESS SPECIFICATIONS

Table 2-1 lists the general set of implantation process specifications included in the MANTECH contract. These are based on extensive NRL experience with implantation of M50 bearing alloy for the purpose of improving its corrosion resistance in the marine (chlorine containing) environment. The dose, energy, and angle requirements arise from the need to build up sufficiently high Cr content (>13 at. %) so as to promote corrosion resistance. Implantation at too high angles from the normal results in excessive sputtering which can limit the retained dose.

Most of the other specifications relate to the need for extreme cleanliness, both during parts preparation and processing. This is important because of the very superficial nature of the implanted surface (i.e., only the first few microinches of the surface is alloyed during the process).

TABLE 2-1. GENERAL IMPLANTATION SPECIFICATIONS

1. Implant energy 120 keV
2. Mass analyzed ion beam is Cr^+ (for bearings), or N^+ (for W C tooling)
3. Dose is typically 2×10^{17} ions/cm^2
4. Ambient vacuum better than 1×10^{-6} Torr
5. Surface temperature less than 250°C
6. Maximum angle of incidence relative to normal is $\pm$ 30°
7. Implant uniformity better than 15%
8. Pilot production level throughput
9. Parts handling in a laminar flow bench
10. Surface cleaning specification
11. No fixture materials that deposit contaminating films

SECTION 3
END STATION DESIGN AND EVALUATION

The first phase of the Ion Implantation Manufacturing Technology Project was solely oriented toward the design of the end station system and workpiece fixtures. Fabrication was undertaken in Phase II, which is coincident with the second year of the program.

The ion implanter end station system is naturally divided into three parts. These are: 1) beam transport, 2) vacuum chamber and support subsystems, and 3) workpiece-handling fixtures. These items will be discussed individually in the following sections.

3.1 BEAM TRANSPORT SYSTEM

The ion beam presented at the exit of the NV-10-160 ion implanter is in the form of an ellipse nominally 0.8 cm wide x 2.54 cm high in size with divergences of 26 x 5 milliradians, respectively. The initial intent of the Spire approach was to reshape this beam spot to a much larger size without creating excessive nonuniformity of beam current. The method selected was to enlarge the beam with magnetic quadrupole lenses and to relieve local inhomogenieties with a drift length which has a perpendicular electric field. The latter is included due to the inevitable local variation in intensity that is characteristic of these high intensity ion beams. The specification on uniformity is $\pm$ 15%. The beam transport components are clearly visible in Figures 2-1 and 3-1.

3.1.1 Magnetic Quadrupoles

Much of the initial design work was performed by Prof. H. Enge of M.I.T., who consulted on this project. The configuration used consists of three lenses, the first two closely spaced and the third separated by about 40 cm. All are mounted on a common frame. This configuration was found to be needed to avoid the introduction of beam nonuniformities. Specifically, the field and geometrical transport parameters are selected to create a beam spot which is dependent only on the beam divergence along the minor axis. This is shown schematically in Figure 3-2. With only one lens there tends to be a concentration of beam in the center of the resultant beam spot at the workpiece.

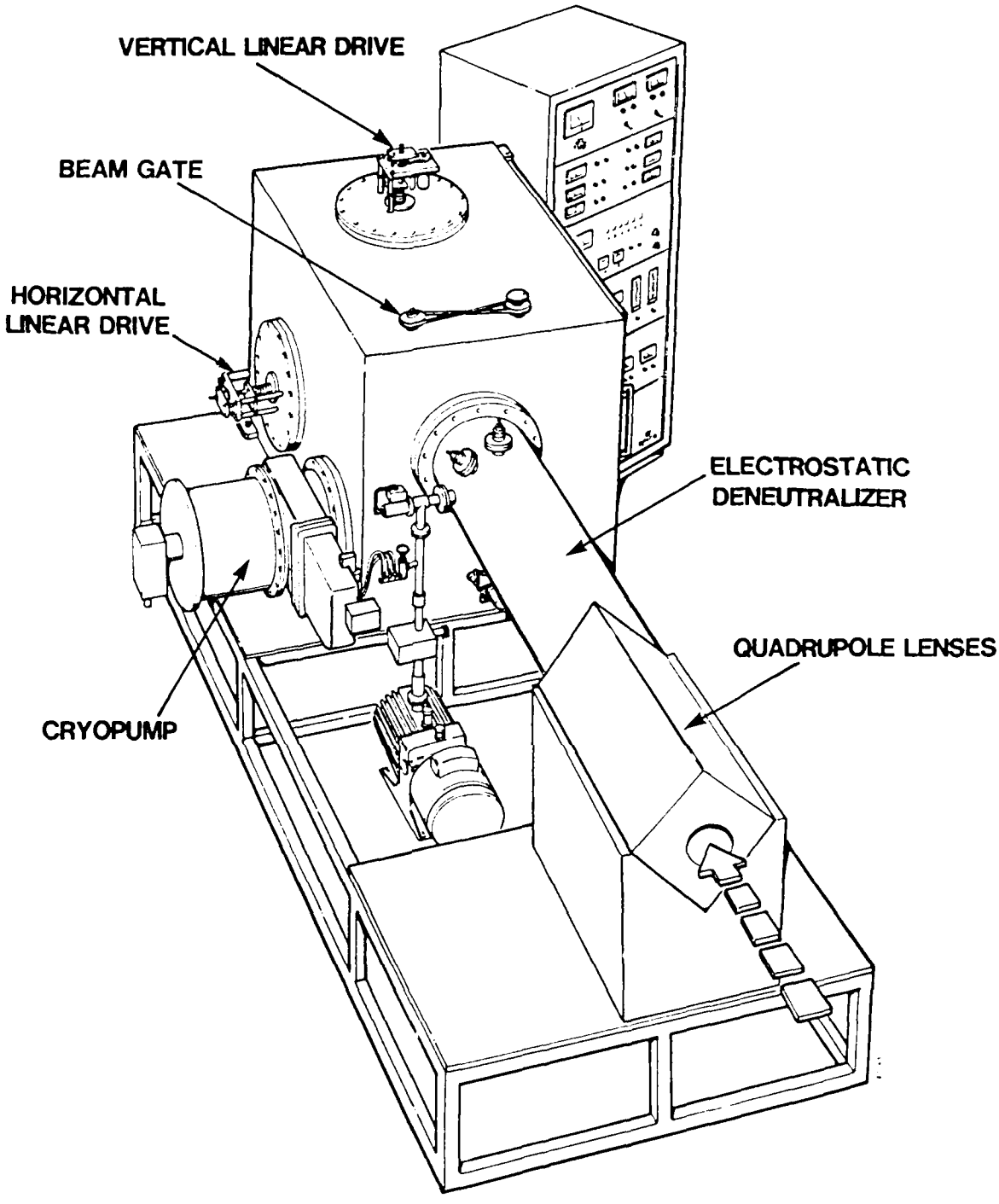

FIGURE 3-1. END STATION SYSTEM.

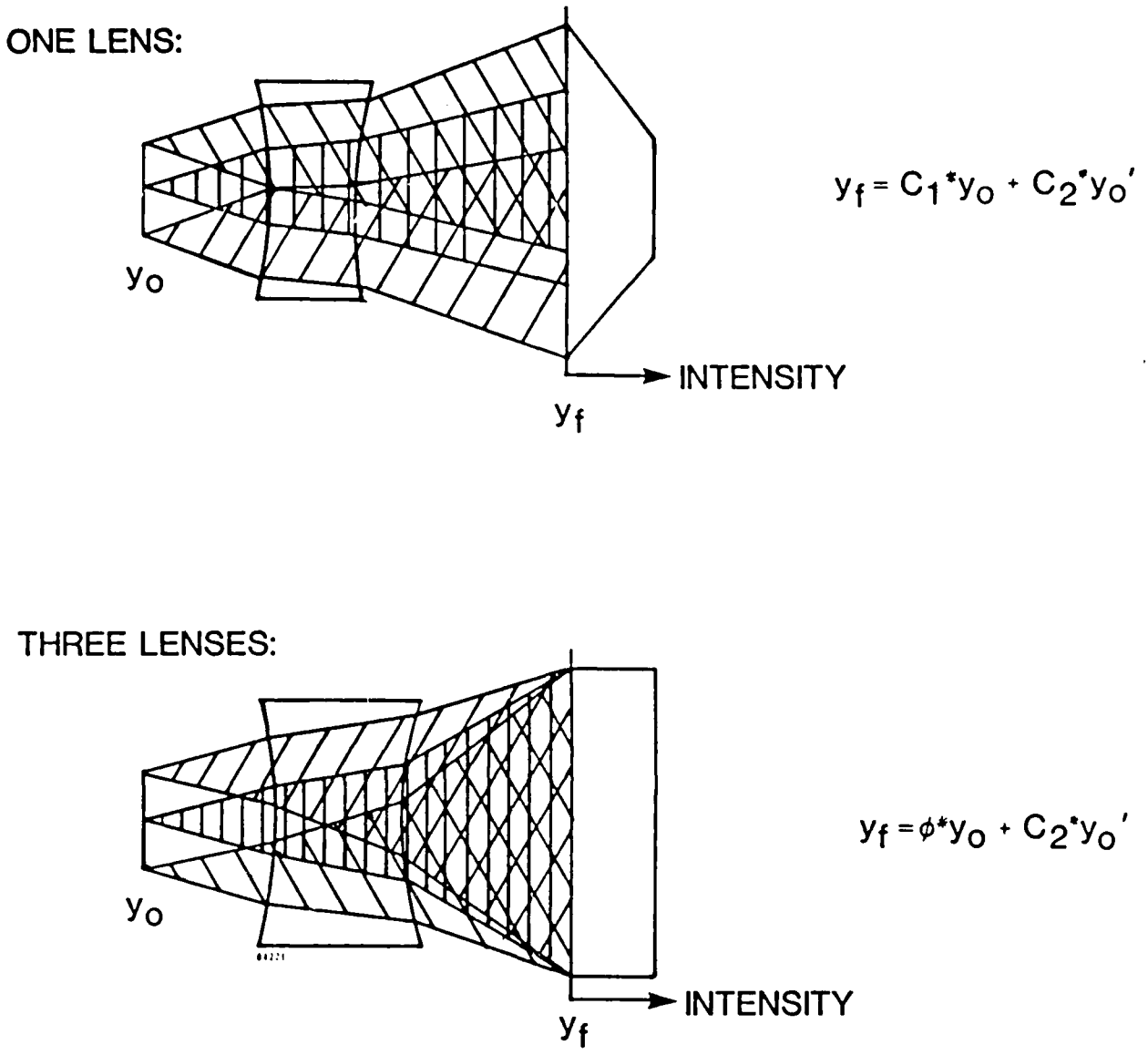

FIGURE 3-2. THREE LENS REQUIREMENT.

With three lenses, it is possible to map any point of the input beam across the entire face of the target. In this way nonuniformities of current distribution are greatly reduced.

The lenses were designed to have considerable flexibility in the range of spot shapes that can be created. With this system most elliptical or circular shapes can be created up to about 14 inches in diameter. Limitations do exist for very heavy nuclides, such as tantalum, at the higher beam energies. Spots of particular interest include circles, 45° ellipses, and a narrow strip beam, about 1" x 12". The ability to vary the spot shape to suit the workpiece was deemed critical to maximize utilization of the beam. The value of the large spots is in the low power density, which reduces cooling requirements and the need to constantly move samples in and out of the beam. This system is thus oriented toward large batches with low-to-moderate, continuous heat loads.

Sample beam transport calculations are shown in Figures 3-3 through 3-5. These correspond to the circular, 45° ellipse, and strip beam cases, respectively. The locations of the three quadrupole lenses are marked, together with the position of the deneutralizer, which is discussed in Section 3.1.2. Each Figure shows two half profiles of the beam. The half labeled "top view" is the horizontal cross section and the lower half labeled "side view" is the vertical profile. For the case of the circular spot, Figure 3-3, the final target spot on the right edge is equally spread on both axes, the definition of a circle. The vertical axis is successively narrowed for the two cases in the other figures.

The calculations of the beam profiles have been performed using a first order beam envelope computer program based on TRANSPORT, a beam transport program which was originally written at Stanford. This code uses linear matrix transformations to predict the beam dimensions and divergence at selected points along the trajectory. Individual particle trajectories are not considered. The code is advantageous in that it is fast and parameters can be optimized to produce required configurations. In its conventional form, however, it cannot predict the effects of space charge in the beam or the more extreme effect of space charge deneutralization which will be discussed next.

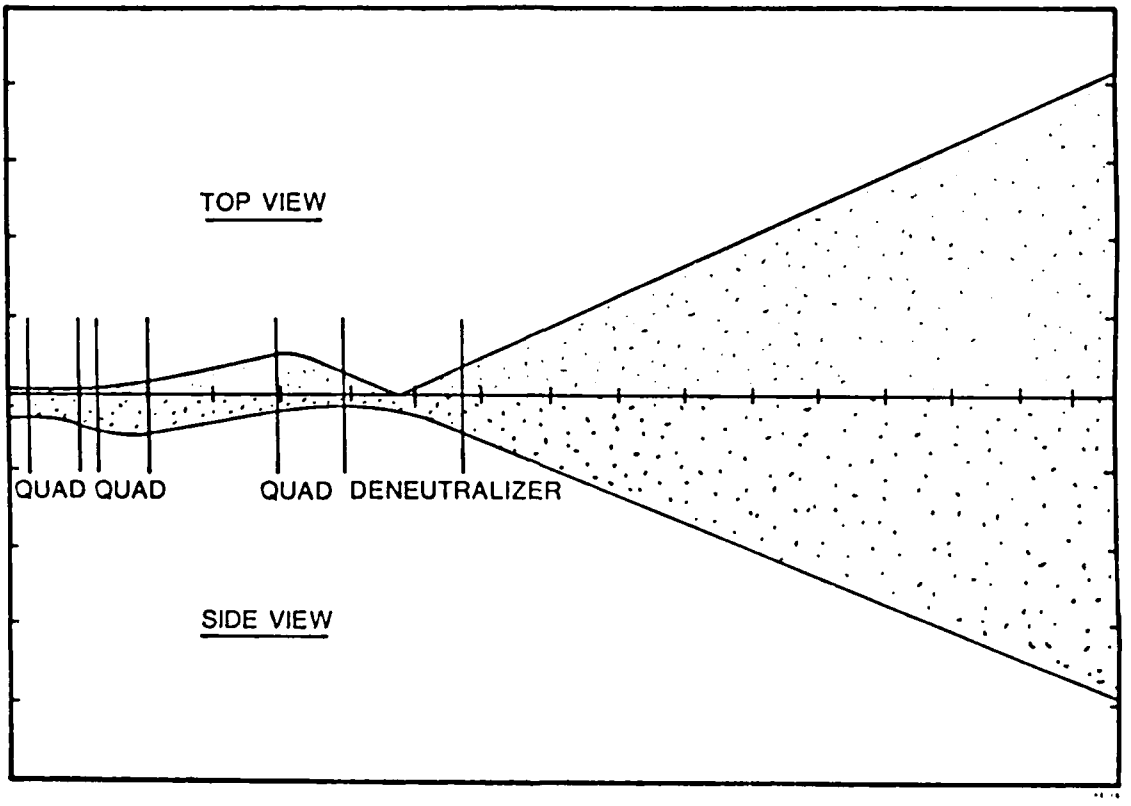

FIGURE 3-3. CIRCULAR BEAM SPOT.

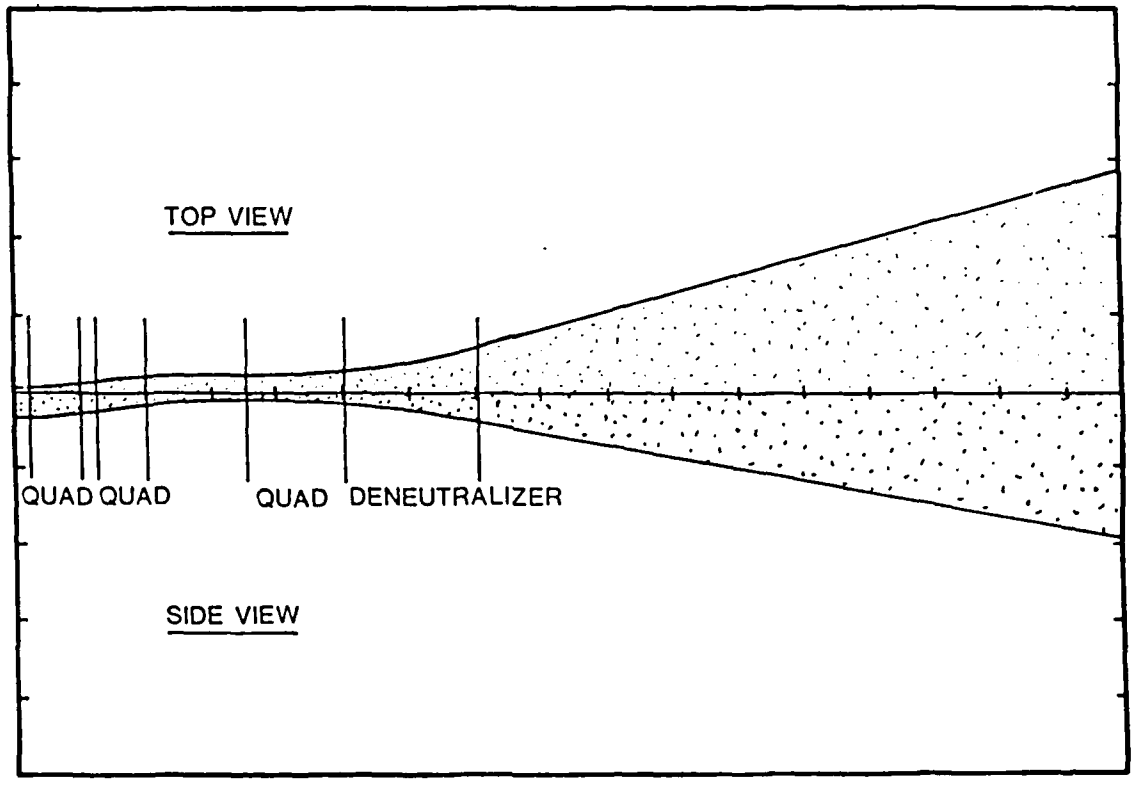

FIGURE 3-4. 45 DEGREE ELLIPTICAL BEAM SPOT.

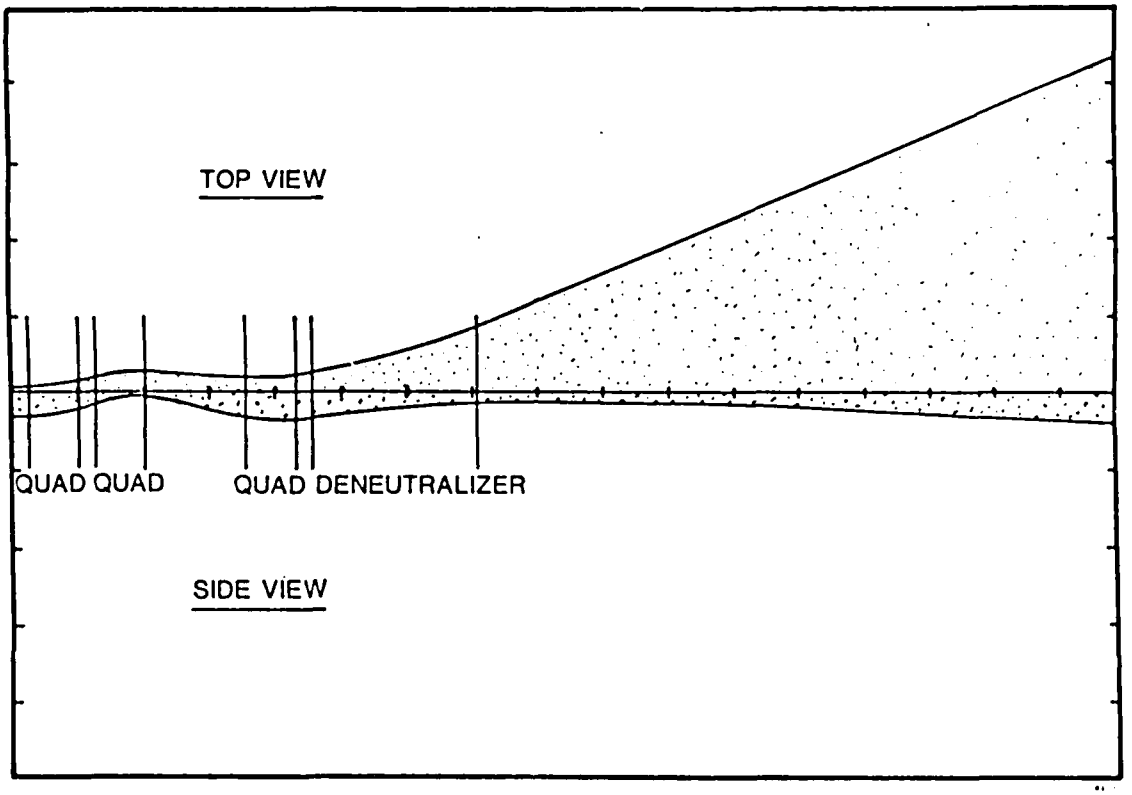

FIGURE 3-5. STRIPE BEAM SPOT.

3.1.2 Deneutralizer/Deflection System

There is a limit to the ability of the quadrupole lenses to produce a pseudo-uniform beam spot. It was therefore deemed necessary to add a supplemental system to improve the beam profile further.

It is well known that high current ion beams possess a sufficient space charge density to cause the beam to significantly expand in diameter during transport. This is due to the mutual repulsion of the positive ions as they travel together in the beam. It is a major effect for slow moving ions (i.e., low energy or high mass ions). In practice, ionization of the background gas provides sufficient electrons to "neutralize" the space charge (i.e., shield the positive charges) and in this manner intense beams can normally be transported. However, any zone in which an electric field is present will sweep away these neutralizing electrons, resulting in an increase in radial velocity and beam enlargement. Generally, this effect is a nuisance often encountered in beam deflection and acceleration systems involving high intensity (milliampere) ion beams.

In the case of the initial Spire approach, it is important to have a large diameter beam and this space charge expansion is not a harmful phenomenon. In fact, the effect is deliberately utilized to cause local zones of higher current density to expand at a more rapid rate, thus further equalizing the current density across the beam spot.

Figure 3-6 shows such a deneutralizing system. The initial design also incorporated beam steering capability as well. There are three pairs of electric field plates with the outer pairs having a reverse field to that of the longer inner plates. The plates are on rails which easily enables them to be repositioned, and separate voltages can be applied to either of the two live rails. The plates are shaped to partially cancel end effects and can easily be replaced with other configurations. Sufficient voltage can be applied to steer the beam up to 7" off axis at the target plane, although only a few hundred volts/cm are needed to effect the space charge deneutralization. The different length plates are used to cancel the steering and offset effects of the perpendicular electric fields.

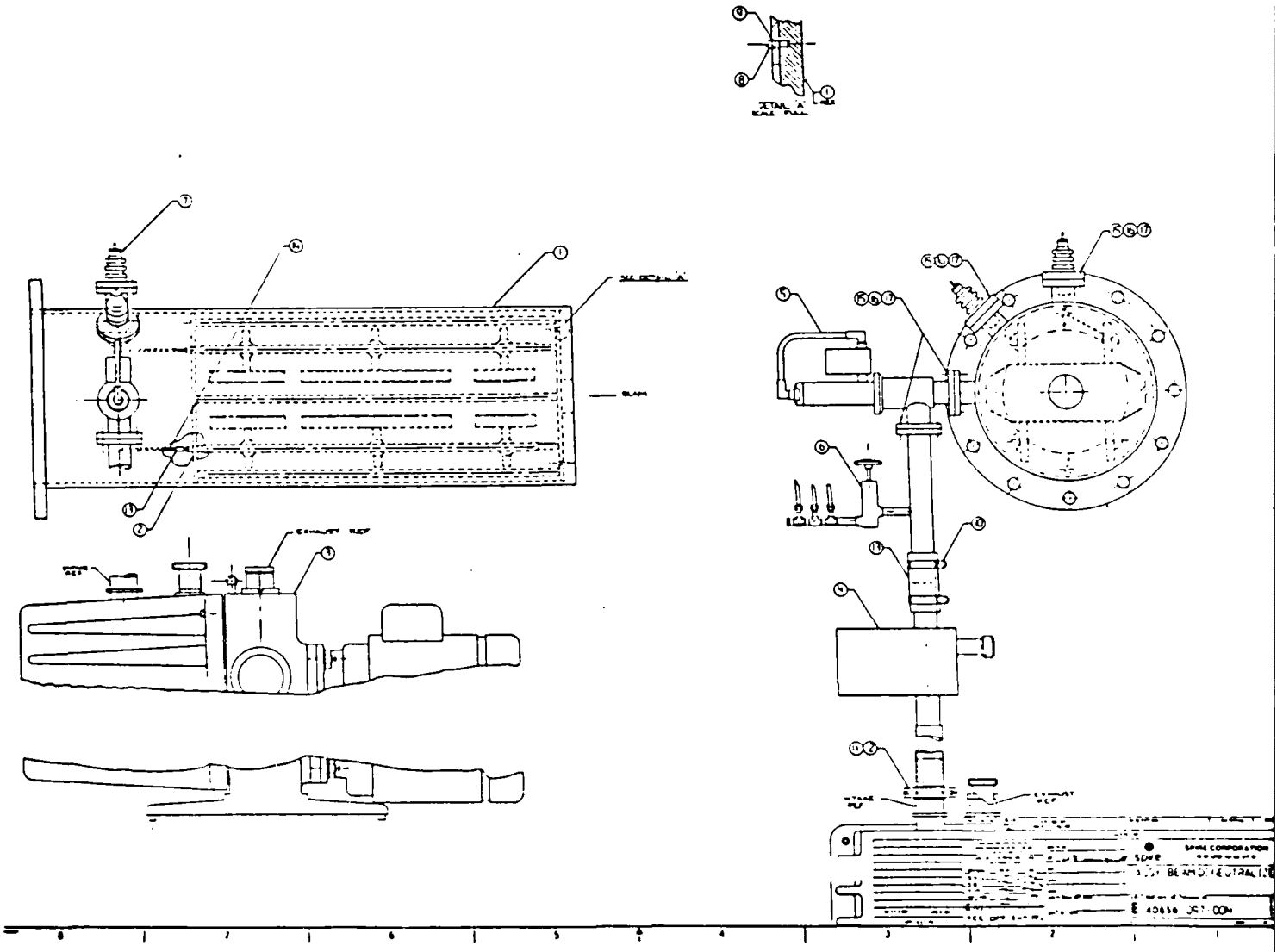

FIGURE 3-6. BEAM DENEUTRALIZATION SYSTEM.

3.1.3 System Modification/Ion Beam Raster System

Although the large area flood beam approach was successfully used on many test and development runs, it was found to have two principal deficiencies; 1) it was difficult and time consuming for the operators to set up totally new beams, and 2) the flood beam shape (elliptical) is less compatible with the basically rectangular fixtures for balls and rollers. In addition, emittance of the ion source was found to vary during source lifetime, thus changing the spot size with time. For these reasons, a two axis beam scanner was developed.

The scanner was a modification of the plate locations used by the deneutralizer system already in operation, so no new hardware was required. Four independent plates provide deflection from the center line, two for each axis (Figure 3-7). Total net deflection capability has been measured at 8 inches from center on all axes, thus yielding a 16 inch diameter masked spot in the middle of the chamber.

This modified system has proven to be quite successful. The tightly focused beam spot needed for scanning is well separated from the beam pipe in the quadrupole lens, and no beam pipe heating from the fringing beam is observed. A 1x2 cm spot can be produced at 120-160 keV. A combination of quadrupole lens settings has been found which results in sufficiently low current density in the region of the deflection plates to permit scanning with no significant beam blow-up due to the space charge effect previously discussed. Setting the scanned area is now much simpler for the operators and professional engineering staff are no longer regularly needed for support.

The power supply for the scanner is derived from the D.C. high voltage supplies used for the deneutralizer system (Figure 3-8). High voltage tetrodes are controlled via optical links from two master oscillators. Left/right deflection from center is generated by driving the plates with two triangle waves that are 180° out-of-phase. Maximum voltage of one wave coincides with the minimum for its partner. Equal voltages correspond to the beam at the center line.

An oscilloscope has been added to the control rack so that an X-Y image of the rastered beam can be viewed. This assists in properly setting the two master frequencies to avoid standing waves (i.e., hot spots). Operation to 23 kV has been tested, although this

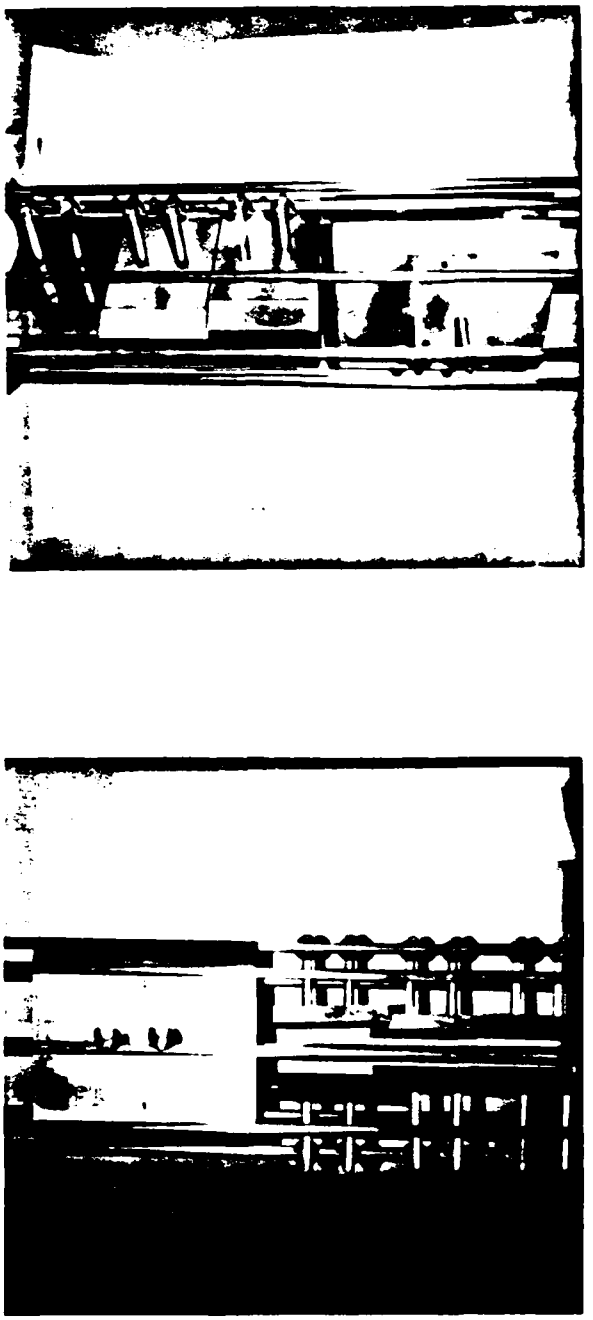

FIGURE 3-7. ELECTROSTATIC SCANNING PLATE ASSEMBLY

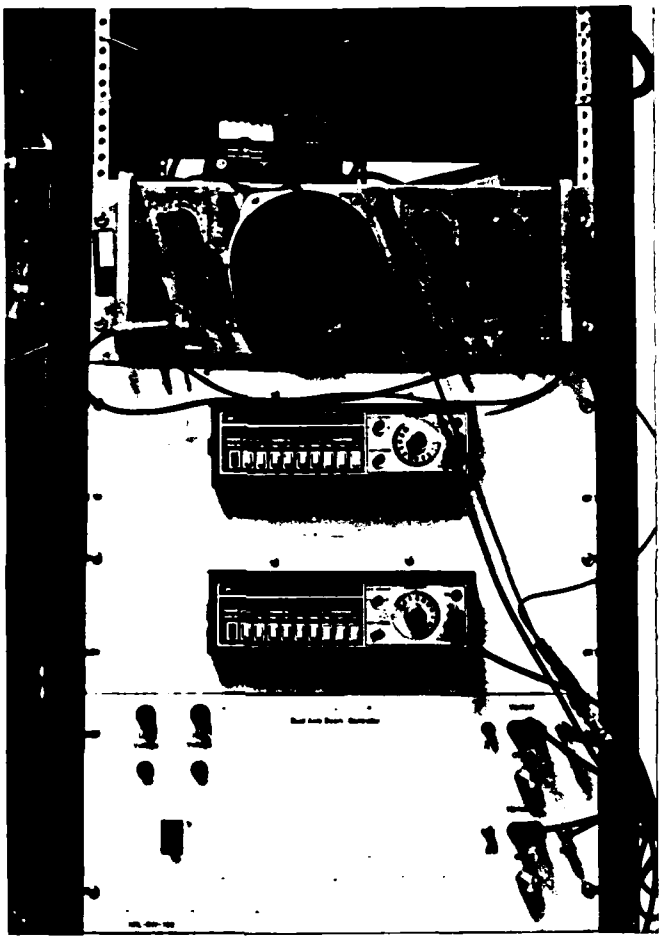

FIGURE 3-8. DUAL AXIS RASTER BEAM SCANNER SYSTEM.

voltage is much more than required for 120 keV ion beams. Load current drawn on the plates is less than 1 milliampere for all 4 plates combined, indicating minimal fringe beam striking the fixtures and little interference with space charge. Normal operation is with 325 and 25 Hz on the horizontal and vertical plates. While the amount of necessary overscan is comfortably low for higher beam energies, a test has indicated that if high beam usage efficiency or uniformity is not a requirement, then 50 keV operation is also practical. The beam spot is about 3 cm x 4.5 cm at this low energy.

Initial tests of this modified raster system allowed further refinement. In particular, the most significant problem encountered with the originally modified raster scan system was caused by the special condition when the applied voltage was momentarily identical on opposing pairs of plates. Figure 3-9 shows the deflection plate geometry as originally installed. Phase-related voltages were applied, as indicated in the bottom of the figure. The phase relation is such that the maximum voltage on one plate

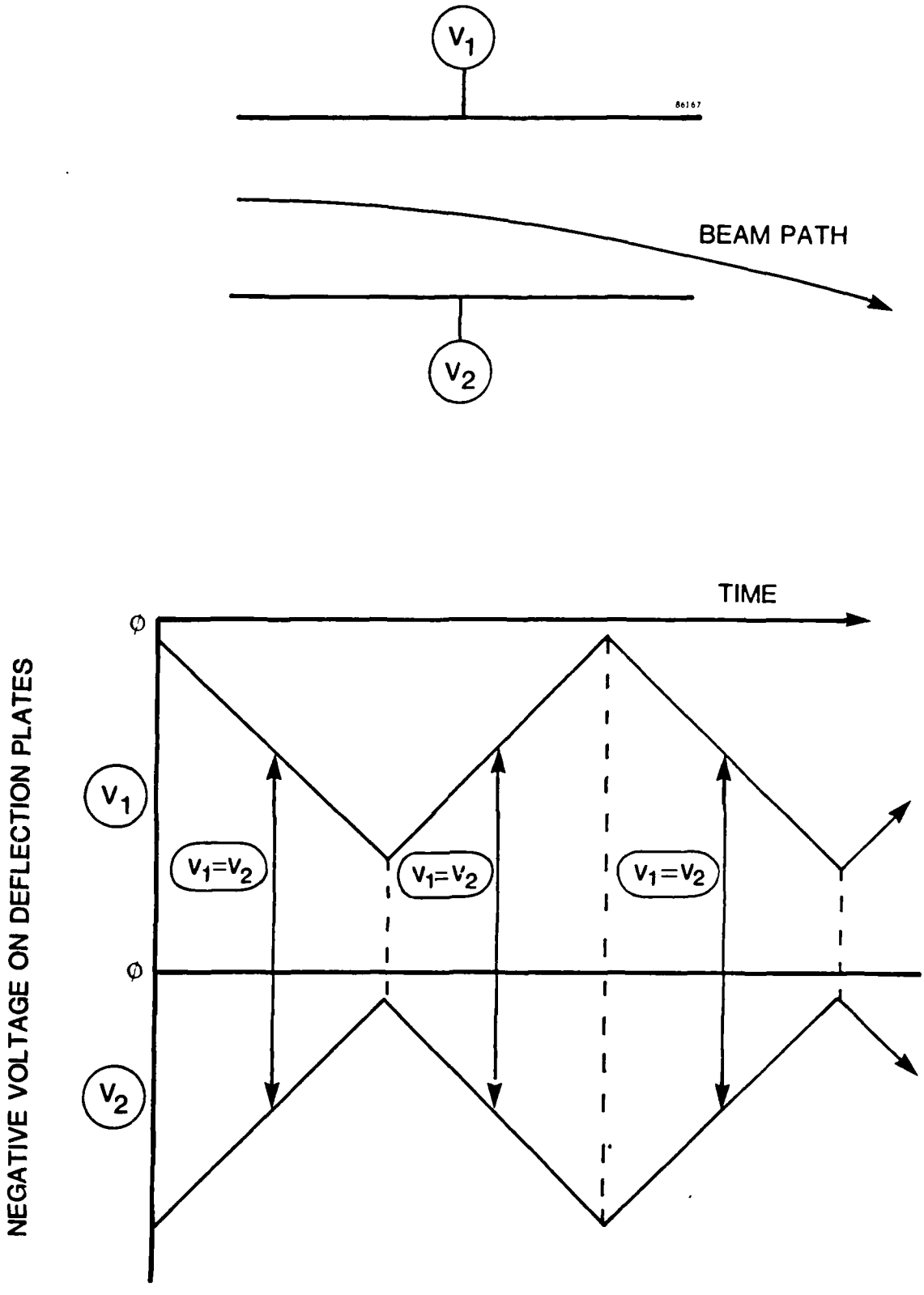

FIGURE 3-9. ORIGINAL DEFLECTION PLATE GEOMETRY.

corresponds to the minimum on its neighbor. In this way the beam is alternately swept back-and-forth through the centerline.

The value of the original plate configuration is in the short length of the plates in order to obtain a given range of deflections. Since a single pair of plates deflects bi-directionally, large total spans are obtained.

The problem encountered occurs at the crossing point between left and right deflection. At this instant when $V_1=V_2$, the space charge deneutralization caused by the electric field abruptly ceases. Despite oscillation frequencies on the order of hundreds of hertz, the beam spot at the target was observed to undergo a change in shape at these crossing points. The sudden shape change resulted in both a non-uniform raster scan and instabilities in the high voltage drive circuit due to the abrupt change in current load.

The problem was solved using the plate geometry shown in Figure 3-10. In this improved design, two pairs of plates are required on each axis. One deflection plate of each pair is always grounded. Although more hardware is needed and higher deflection voltages must be employed for a given effect because of the shorter plate length, the new version has the advantage that space charge deneutralization is always constant. Tests have shown that beam spot shape no longer changes and the high voltage drivers are not being loaded down.

The new design depends on the fact that space charge deneutralization takes place above a threshold electric field strength. The effect of sweeping out electrons from the beam path changes little with increasing applied field after the threshold has been passed. This newer system can operate with deflection voltages up to 20 kV, about double the previous design.

The system has been tested with 120 keV chromium and 150 keV titanium ions and has been found to function as predicted. It can produce a rectangular spot as used for the implantation of outside races (Sect. 3-2-3) with good success. Setup time is minimal and no run-time anomalies were observed.

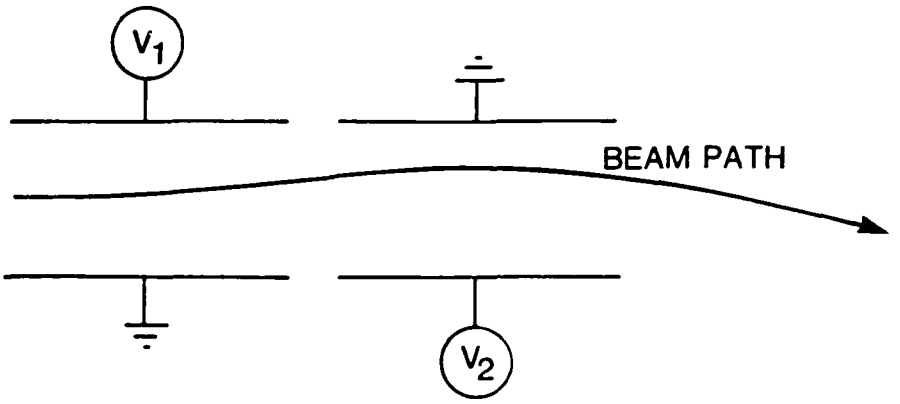

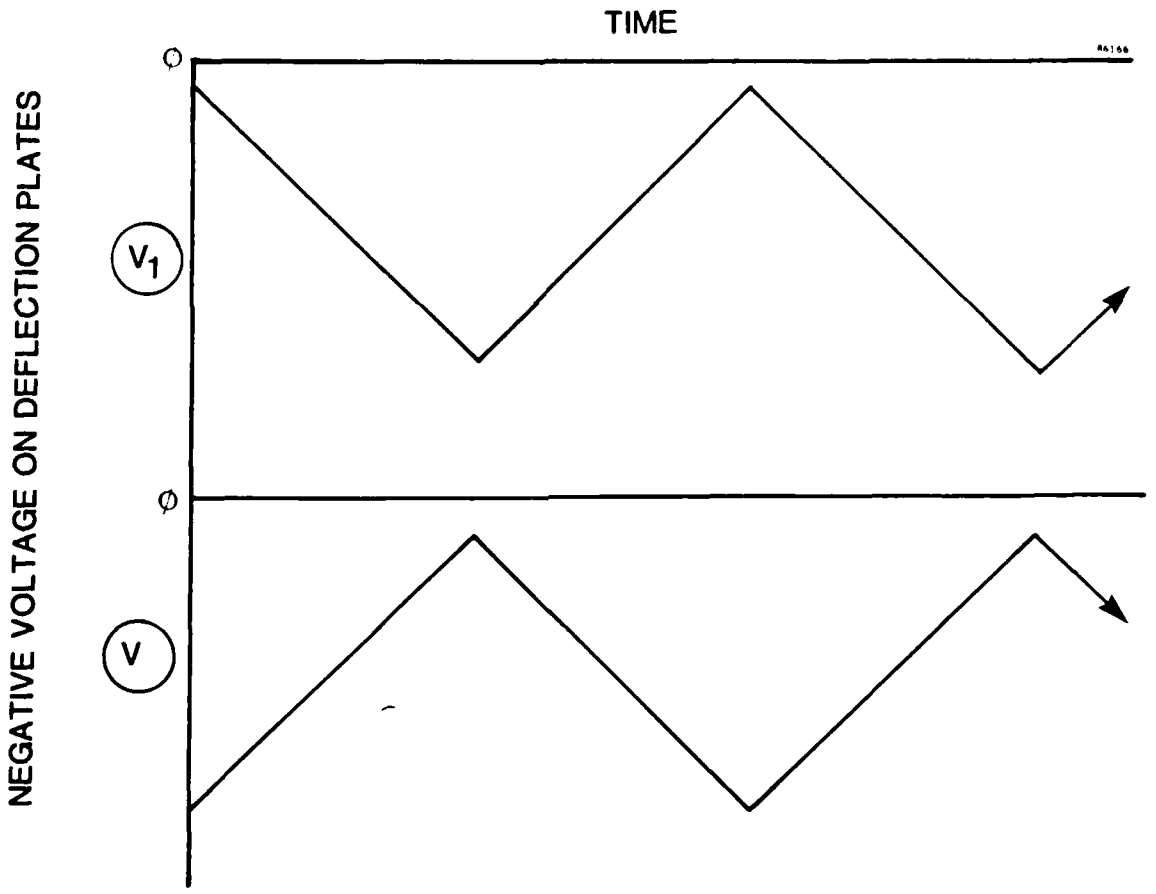

FIGURE 3-10. MODIFIED DEFLECTION PLATE GEOMETRY.

3.2 END STATION/WORKPIECE FIXTURING

Design work on the ion implanter end station consisted of detailing existing designs and creating new layouts based on the concepts outlined in the December 1983 Technical Interface meeting with NRL.

3.2.1 Quadrupole/Target Chamber Support System

After the completion of the consultant's (Prof. H. Enge of MIT) work on the specification of the quadrupole lenses, the support frame for the quadrupole and target chamber was designed.

The quadrupole lenses could have been mounted on a common magnetic frame, or alternately the third, downstream lens could have been mounted as a separate unit.

The advantages of the fixed common frame are:

1. Minimimal alignment problems
2. Less expensive construction

The advantages of two separated units are:

1. Design flexibility
2. The downstream lens can have a larger bore size because of the larger beam in this area
3. For a swept beam, the third lens is not required and could be eliminated

After weighing those alternatives, it was decided that the main vacuum chamber and the quadrupole should both be supported on a common frame (Figure 3-11). The lenses have an additional support structure to adjust for the height difference. The frame, lenses, and vacuum box are fixed spatially.

The left-hand frame section in Figure 3-11 houses the bulkier power supplies for the quadrupoles (Figure 3-12), high voltage for the steering plates, with the control panel for these units being located elsewhere in its own rack (Figure 3-8). The scanning plate assembly (Figure 3-7) is removable and is supported only by its connections at the ends. The frame section under the steering plates houses the roughing pump (Figure 3-1).

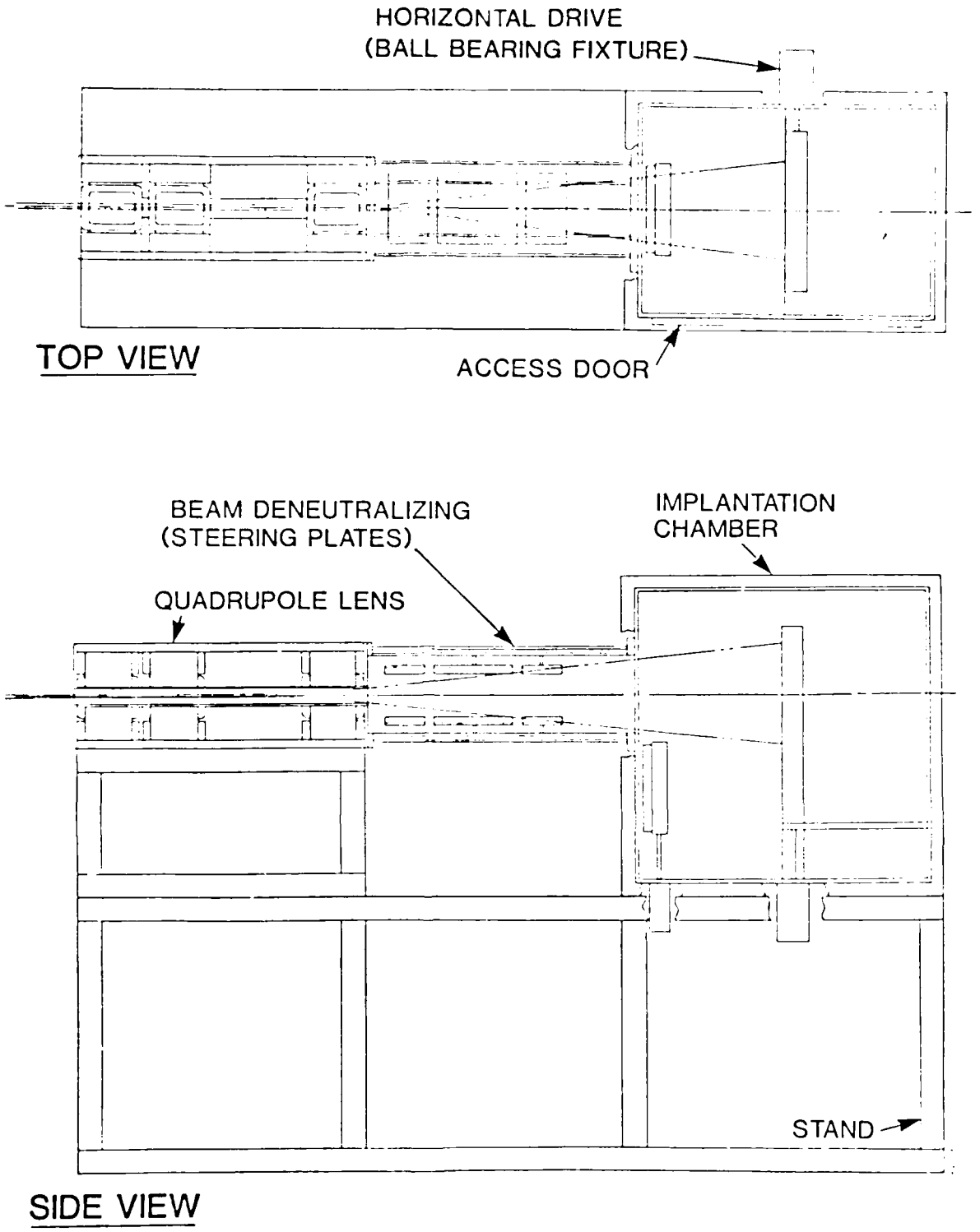

FIGURE 3-11. SUPPORT STRUCTURE FOR THE END STATION.

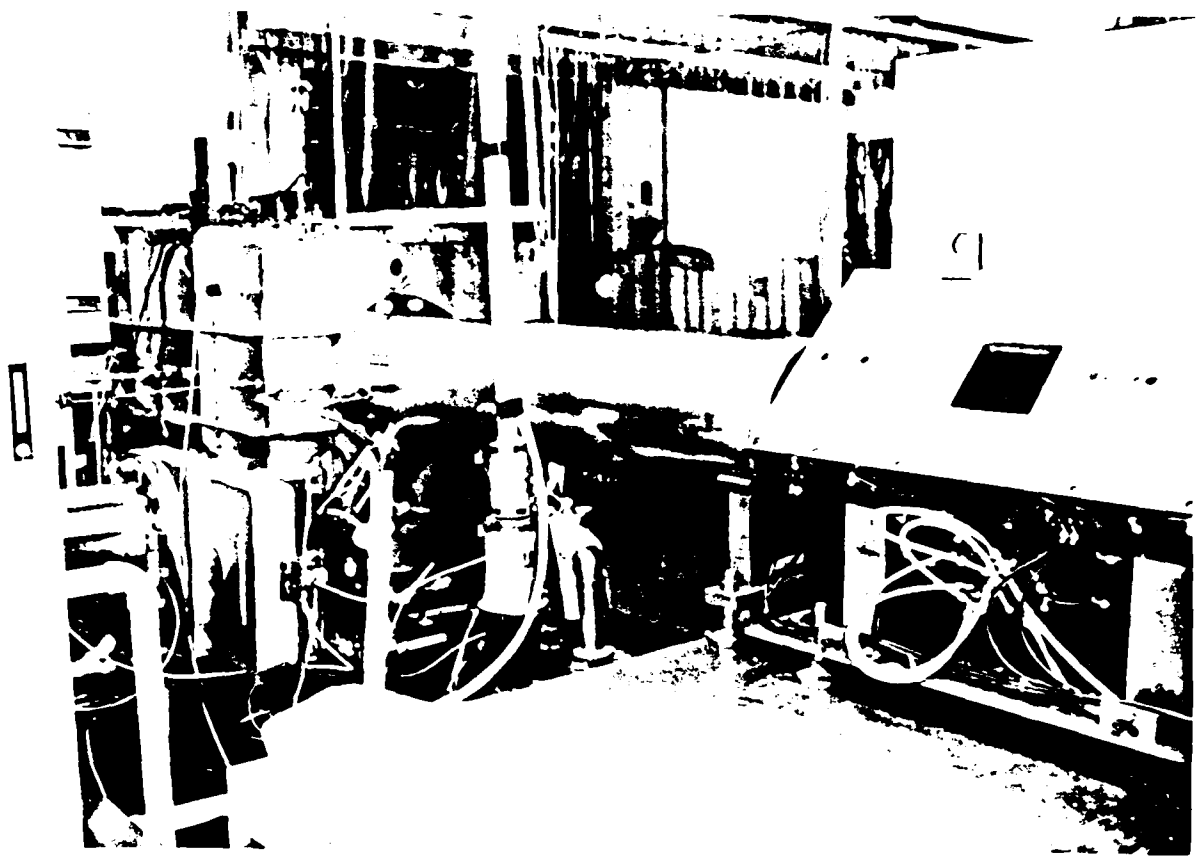

FIGURE 3-12. PHOTOGRAPH OF QUADRUPOLE LENS AND TARGET CHAMBER (REAR VIEW).

Early beam transport calculations indicated that several benefits could be obtained by increasing the length of the steering plate section of vacuum pipe. These advantages were:

1. Decreases in required quadrupole magnetic fields
2. Smaller aperture in the quadrupoles
3. Less angular divergence of the beam at the workpiece (i.e., closer approximation to a parallel beam, which lowers spatial dependence of current density)
4. Smaller beam envelope in the steering plate, which gives more defocusing and greater steering capability for a given voltage on the plates

The disadvantages are:

1. Larger volume to evacuate
2. Longer structure to fit in the available building space

Both of these disadvantages were considered to be relatively unimportant with respect to the benefits. Since pumpout time is largely dependent on total surface area rather than volume, the increase was not expected to be significant and the beam pipe length was made long. Subsequent experience has justified this decision.

3.2.2 Target Chamber/Vacuum System

The primary considerations involved in choosing a design for the target chamber included:

1. Sufficient room to accommodate workpiece fixturing and feedthroughs
2. Minimal surface area to minimize pumpdown time
3. Observation of the beam and mechanical operations
4. Ease in mounting fixtures and rapid changeover time

A rectangular stainless steel chamber (36"x36"x36") with external welded ribbing was selected to satisfy all of the aforementioned considerations. One entire side serves as a door and contains a large (12" diam.) viewport. Figures 3-13 and 3-14 show various views of the chamber.

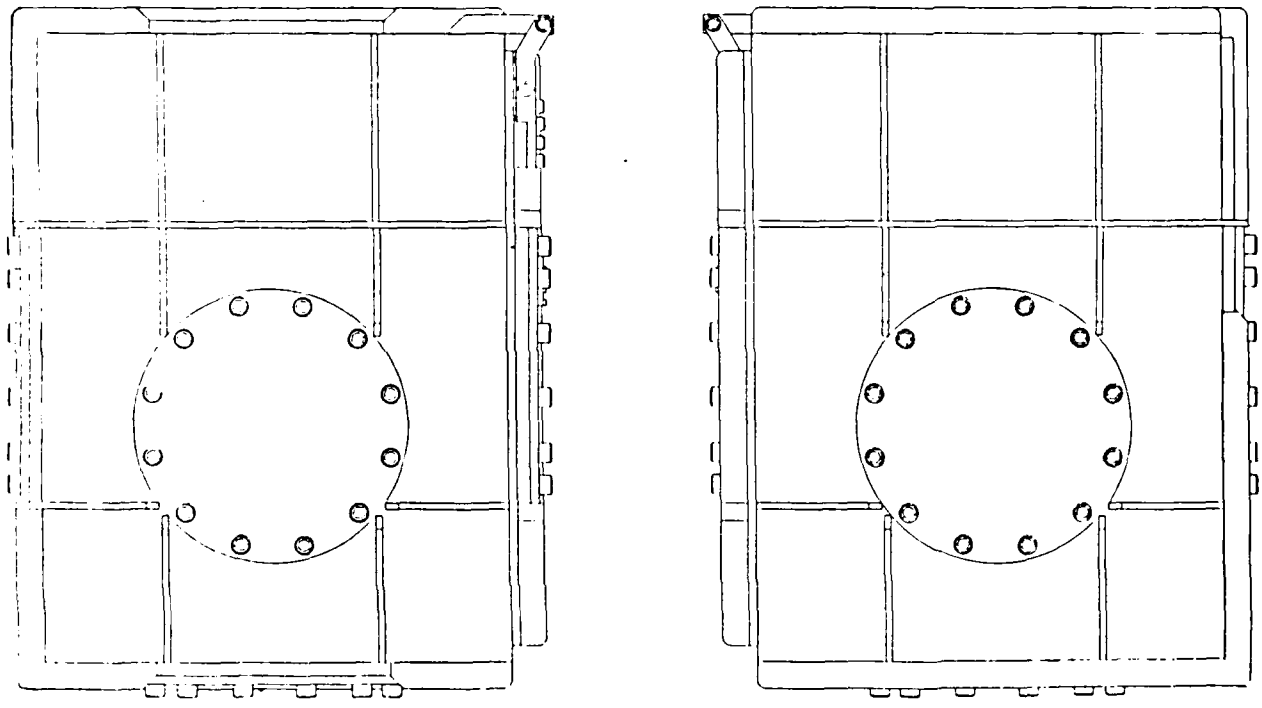

FIGURE 3-13. VACUUM CHAMBER (TOP (L) AND BOTTOM (R) VIEW).

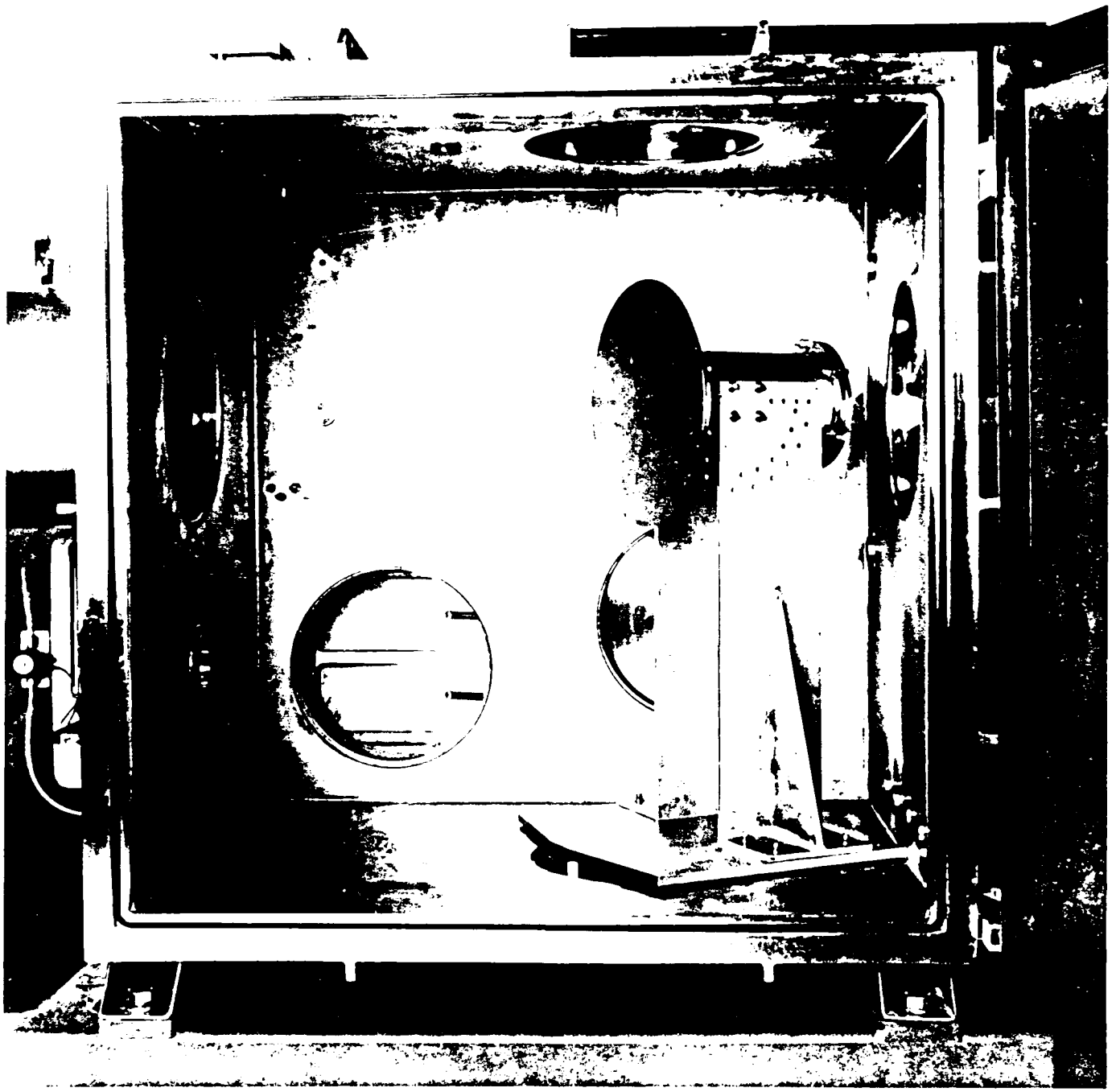

The vacuum subsystem consists of the vacuum enclosure and pumping systems. The specifications require a clean vacuum of 1×10^{-6} Torr to be maintained. This requirement has necessitated a general use of stainless steel components with a minimum of organic insulators and seals. Workpiece-handling fixtures with many "gassy" parts are generally placed inside air-filled enclosures (e.g., rotary drive system) to minimize the evolution of undesirable vapors.

There are two pumps attached to the vacuum chamber. A large, well-trapped mechanical pump is used to rough the volume to the 50 micron level in about 5 minutes. A 10" cryopump is used for the final pumping stage. These pumps are in addition to the two cyropumps on the beam transport line of the implanter.

3.2.3 Workpiece Handling Fixtures

The workpiece handling fixtures were designed to accommodate as large a variety of parts as possible, consistent with the primary goal of implantation of bearing components. The key specifications relating to these fixtures include: 1) maximum angle of beam incidence off normal is 30°, 2) maximum surface temperature is 250°C, and 3) uniformity of dose is $\pm$ 15%.

These specifications significantly constrain the design, particularly for the spherical balls, and result in some loss of beam utilization. The following sections describe how some of the problems have been solved for each component based on the the beam transport system.

Rotary Drive

Design of the rotary drive system is shown in Figure 3-15. It consists of an air-filled enclosure whose axis may be tilted to a variety of angles between vertical and horizontal. The drive has continuous rotation with in-line liquid cooling provided to a large platter such as shown in Figure 3-16 for outer races of bearings. Workpiece-specific holders are attached to this platter and heat is transferred by means of a soft, deformable foil such as indium which acts as a thermal coupling. A ferrofluidic feedthrough was originally used for the rotary seal to maintain the clean vacuum, and was subsequently replaced by a double O-ring rotating seal with differential pumping between the seals.

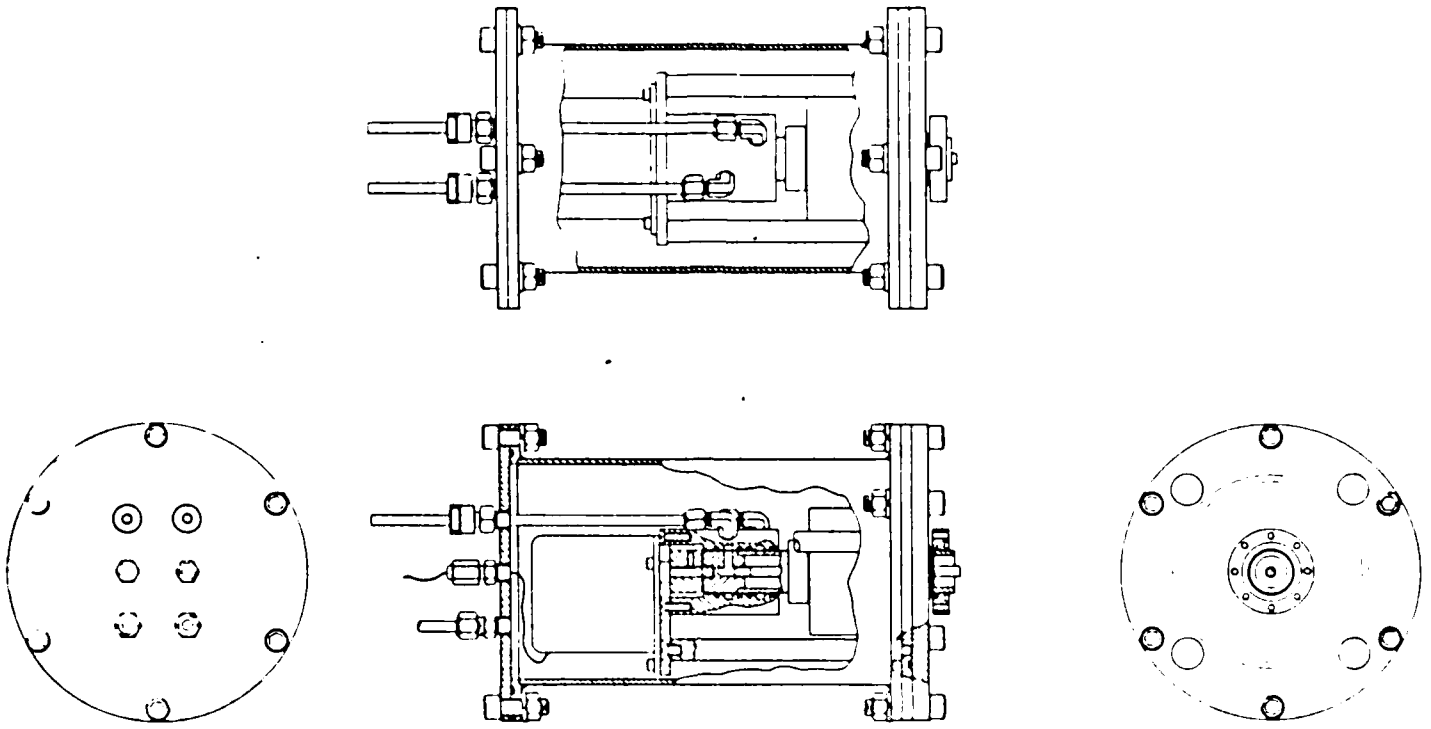

FIGURE 3-15. ROTARY DRIVE MECHANISM.

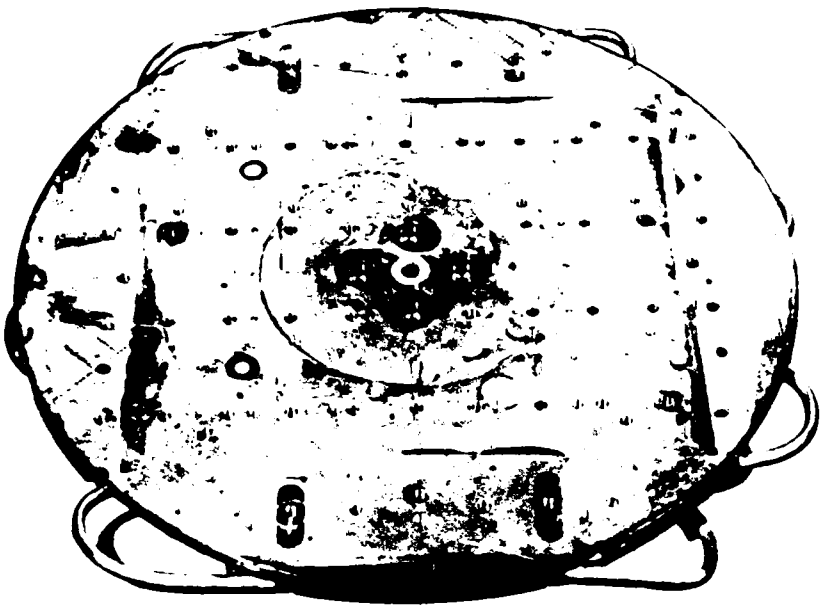

FIGURE 3-16. WATER COOLED PLATEN.

The drive is mounted on supports which permit flexibility in positioning. Besides the tilt system, there is also an adjustment for pivot axis to accommodate different part sizes as well as a height adjustment. Finally, the entire assembly can be turned about a vertical pivot in the chamber floor to permit a second rotation axis, as seen in Figure 3-17. This latter axis is useful when implanting workpieces that contain channels or grooves, such as the races of roller bearings.

The rotary drive supports have been designed to permit rapid modification if this is ever required. New pivot angles, offsets, and the like can be installed by simply drilling appropriate guide pin holes in the support plates.

The rotary drive platter is intended for use with outside races, punches, and any components with complex geometry. It is also useful for flat surfaces and inside races. The only workpieces that do not use this unit are the rollers.

Outside Race Holder (See Figures 3-18 and 3-19)

The plate for outside races is a combination clamp/foil mask assembly sandwiched on a standard base plate for easy transport. Approximately 16% of the race surface is exposed at any given instant. As the platten is rotated the beam can reach the complete inside circumference.

This fixture is a good example of the use of the variety of beam spot shapes obtainable by raster scanning. The tilted platter with races presents an elliptical profile to the beam, a shape which can be readily scanned by the beam transport system.

Inside Race Holder (See Figure 3-17)

The inside races are mounted on a common cooled shaft from the rotary drive. A fixed foil mask is located upstream to maintain the 30° angle of incidence specification. The ion beam is focused down to a horizontal strip for this configuration. Implantation can be performed either at normal incidence (spherical bearing races) or at 30° off normal incidence (channeled roller races). The latter is needed to provide ions to implant the side walls of the channels.

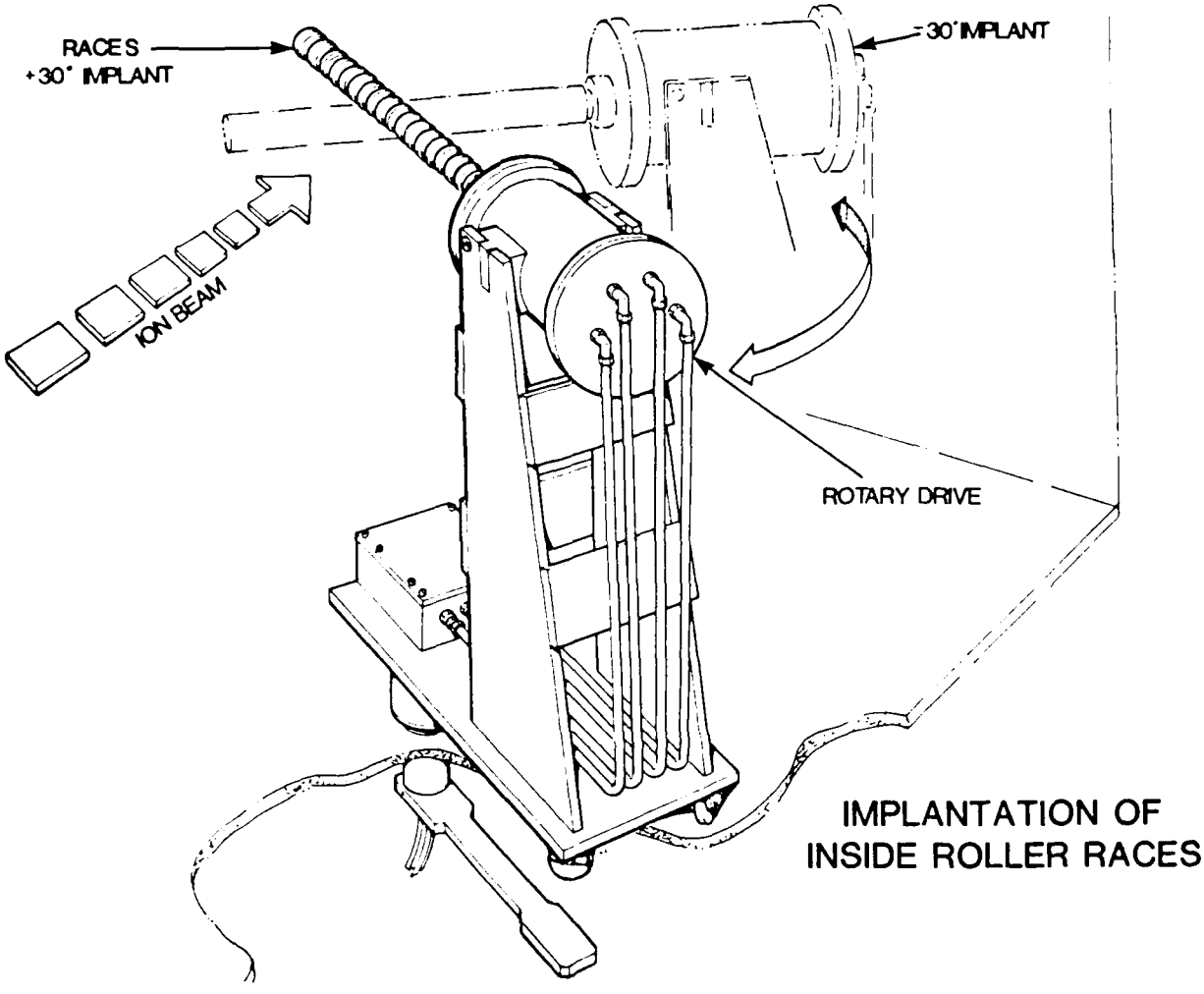

FIGURE 3-17. ROTARY DRIVE SYSTEM WITH INSIDE RACES.

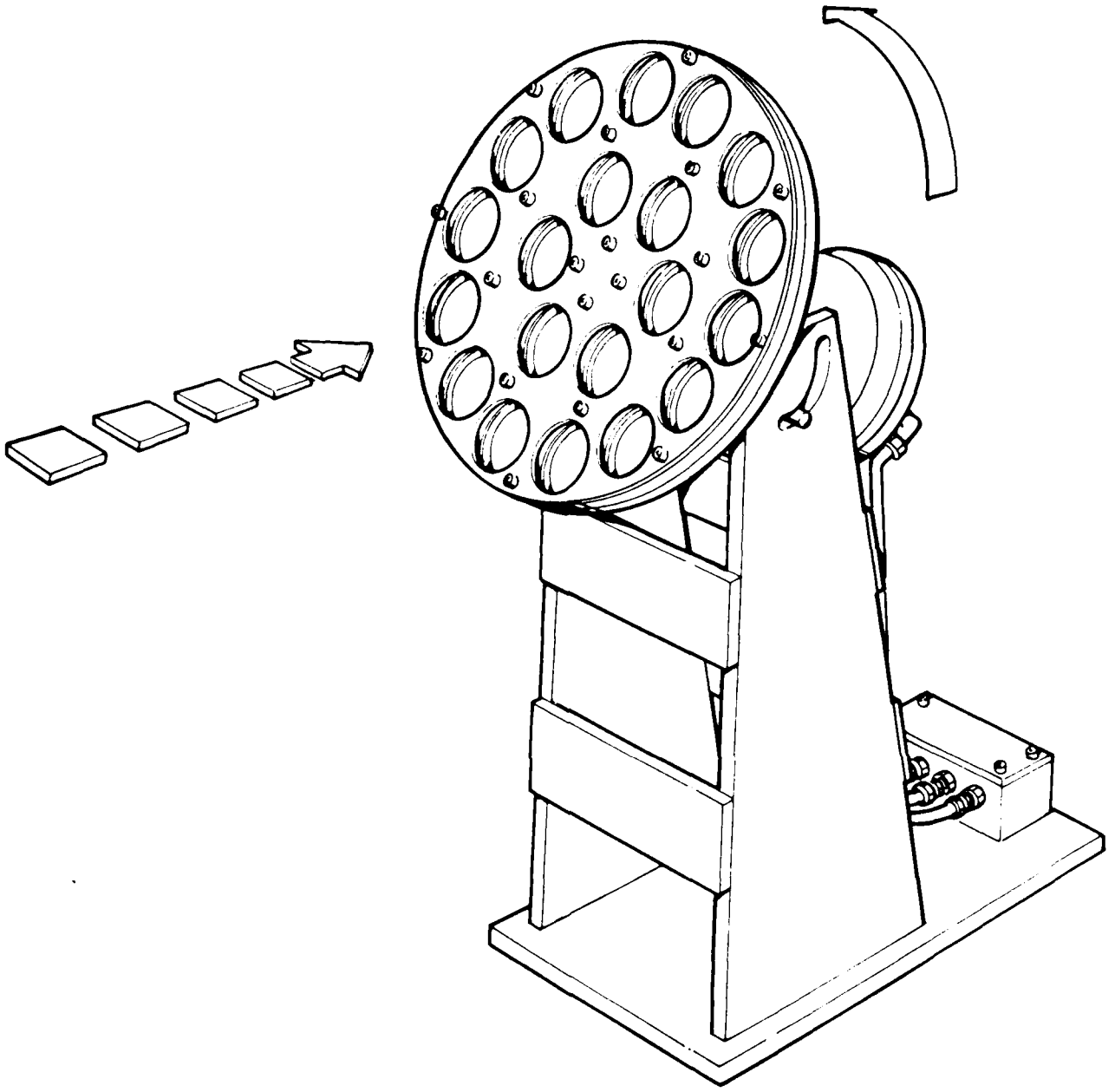

FIGURE 3-18. CUTSIDE RACE PLATTER MOUNTED ON VARIABLE ANGLE DRIVE.

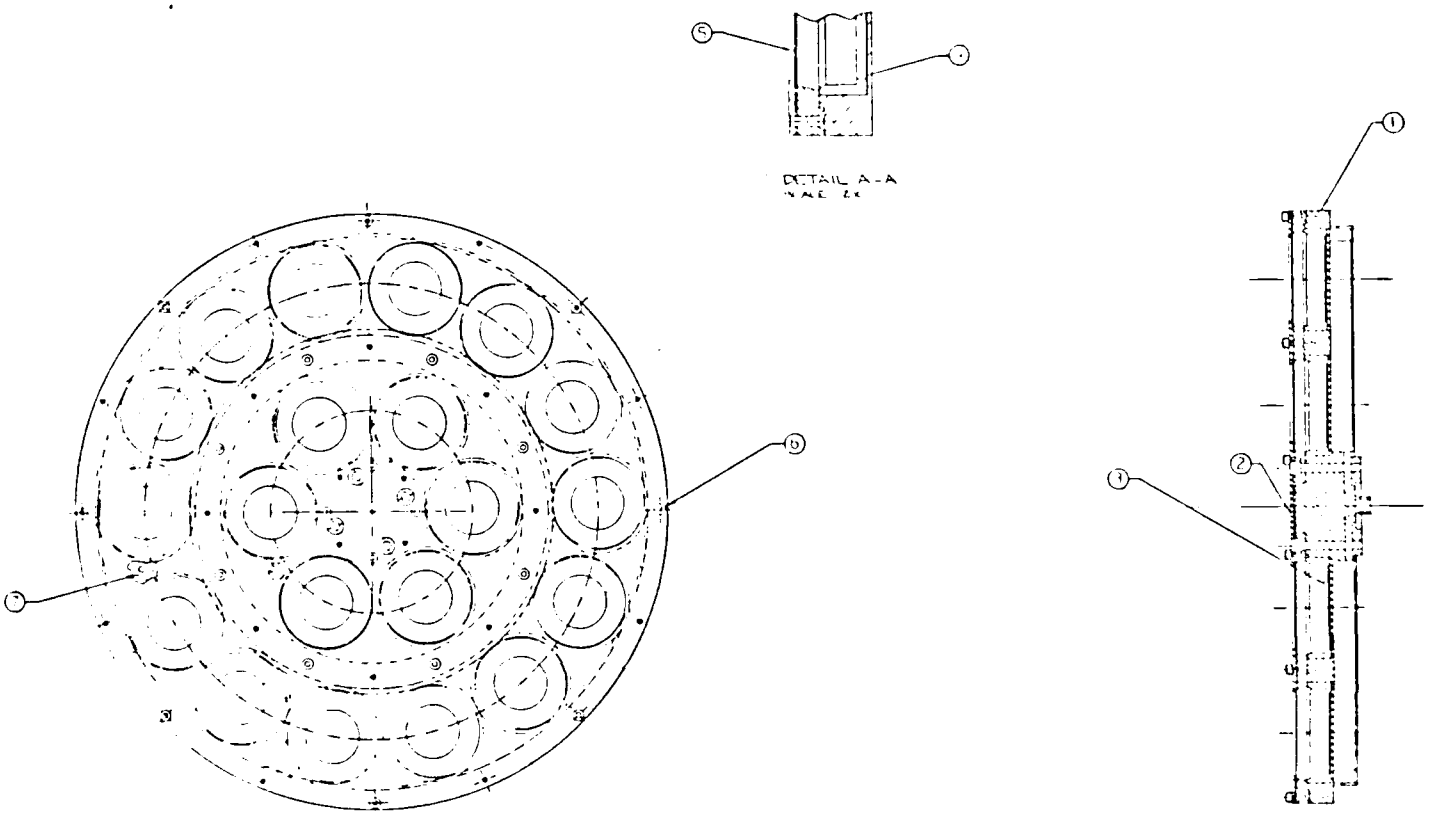

FIGURE 3-19. OUTSIDE RACE HOLDER.

Ball and Roller Drive

Figures 3-20 and 3-21 show the initial design intended for moving cylindrical rollers or spherical balls in order to implant all surfaces uniformly and to adequately heatsink them. It consists of two perpendicular linear drives, each capable of independent motion.

Initial scaled-down trials of this concept for implanting balls or rollers showed that the nickel foil was able to withstand the flexing accompanying ball movement. However, long term motion of the ball platter on a large size (14") platen resulted in ultimate stretching and subsequent failure of the Ni foil. In addition, it was found that the holddown strength of the electromagnet could be improved by employing a much smaller and lighter array of permanent magnets as a holddown system within the vacuum chamber. This array was used to ensure that the rollers had adequate frictional force to move within their holder. Figures 3-22 to 3-23 show the fixtures used to hold the gearbox rollers.

The final arrangement used for M-50 balls is shown in Figure 3-24. It consists of a close packed array of holes in a stainless steel plate clamped to a water cooled platen (Figure 3-16). A tantalum mask in front of the ball-holder limits the exposure angle to $\pm$ 30°. A 5° offset wedge between the vertical platen and rotary drive ensures a periodic forward/backward movement in conjunction with sideways rolling for uniform implantation. By employing large numbers of balls and using a large scanned beam it is possible to limit ball temperature to 250°C and still achieve reasonable throughput (Section 5.2).

3.3 ION IMPLANTER PERFORMANCE

The NRL choice for the implanter was an Eaton NV-10-160 modified ion implanter shown in Figure 3-25 shortly after installation. Since that time several other pieces of equipment have been added, such as the beam scanner unit and an overhead laminar flow curtain to ensure cleanliness.

NICKEL FOIL COOLING SYSTEM

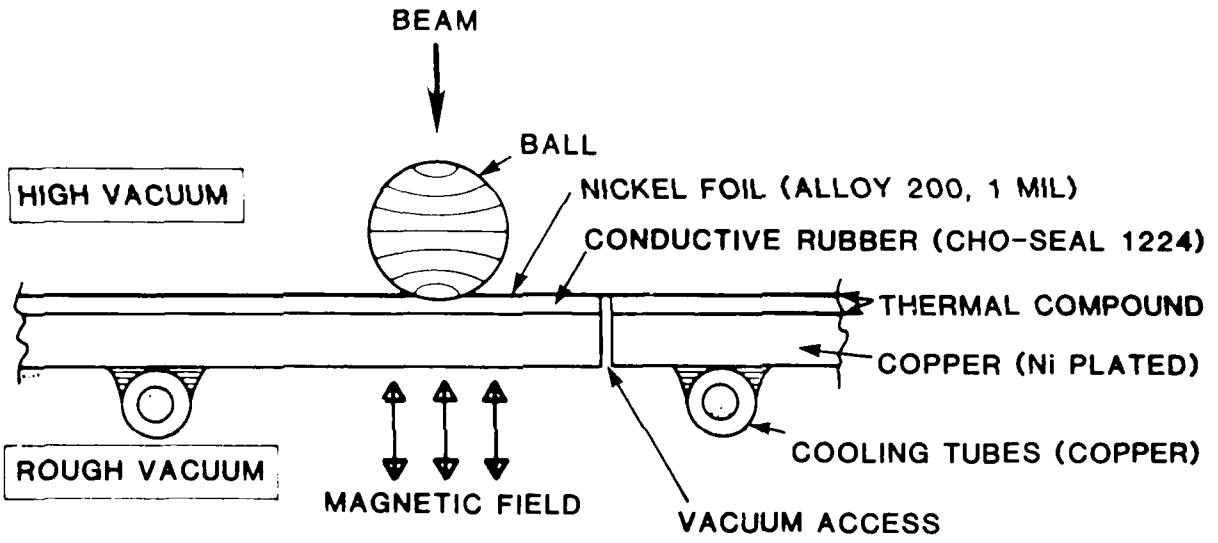

NOTES:

- SCALE: 2X
- BALL SHOWN AT 1000 GAUSS FIELD PULL-IN DEPTH (6 MILS or 10%)
- COOLING LIMITED BY RUBBER LAYER THICKNESS/CONDUCTIVITY

FIGURE 3-20. BALL/ROLLER COOLING/CLAMPING CONCEPT.

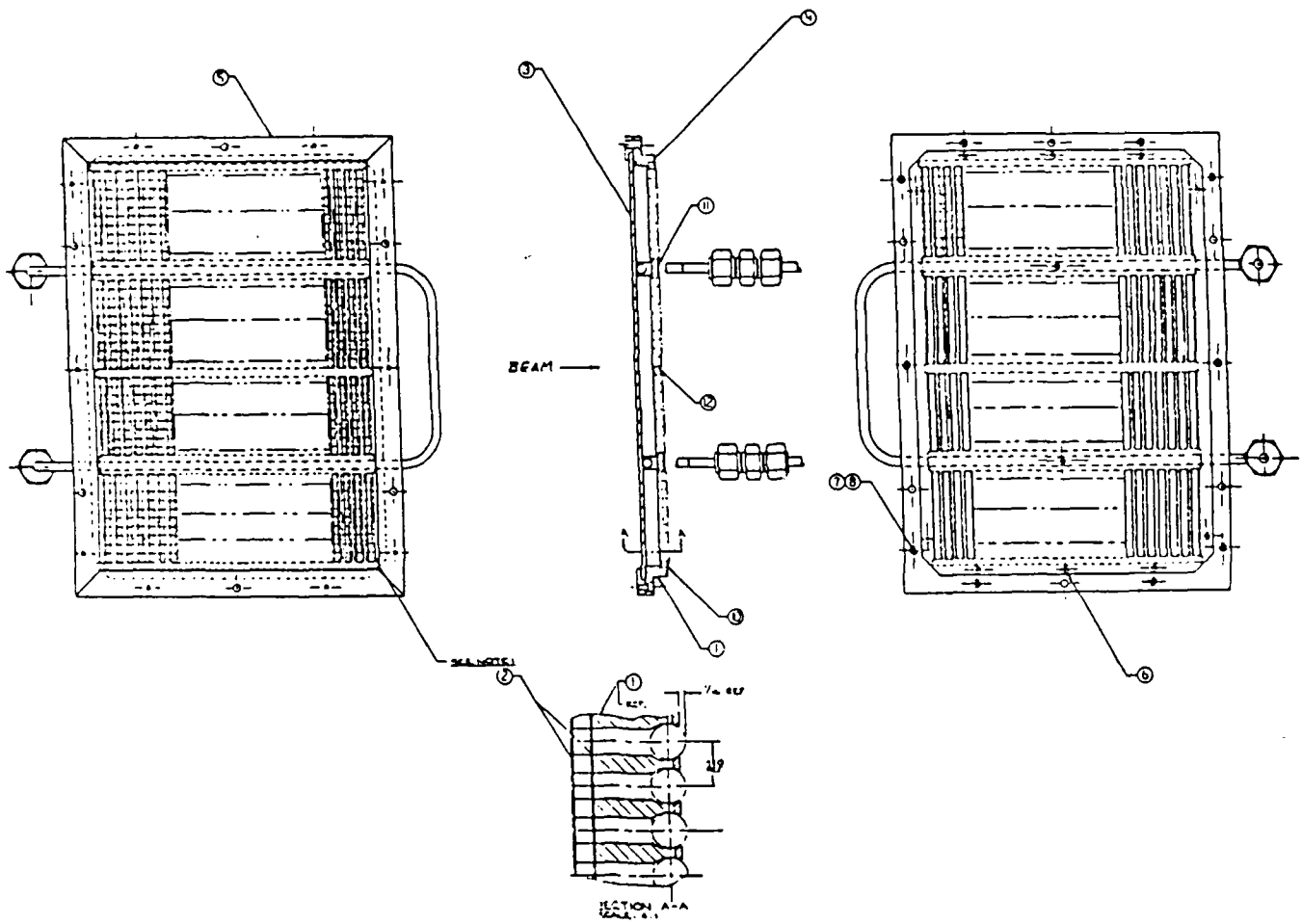

FIGURE 3-21. BALL/ROLLER WORKPIECE FIXTURE.

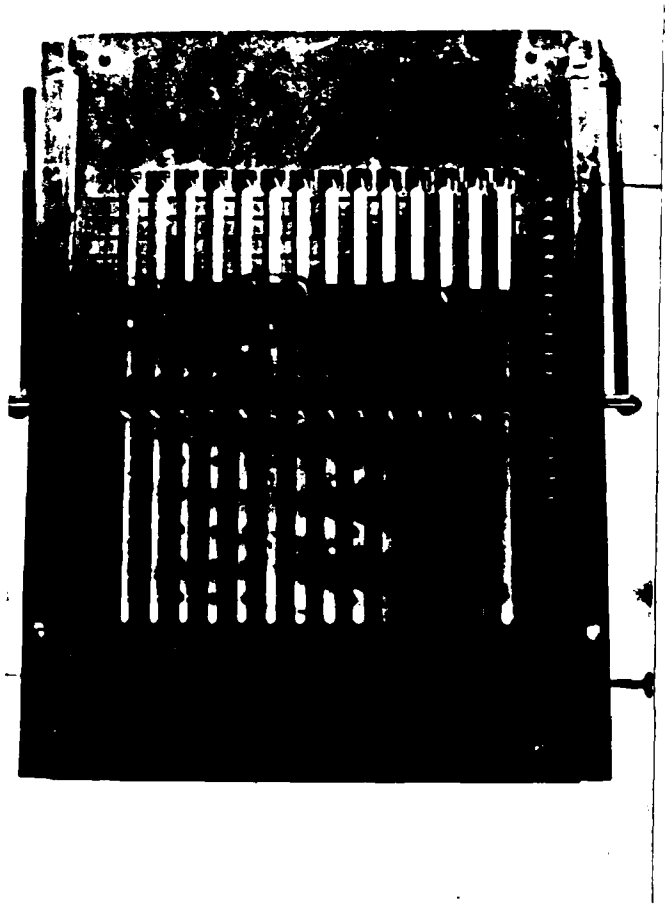

FIGURE 3-22. FIXTURE FOR ROLLER SIDES.

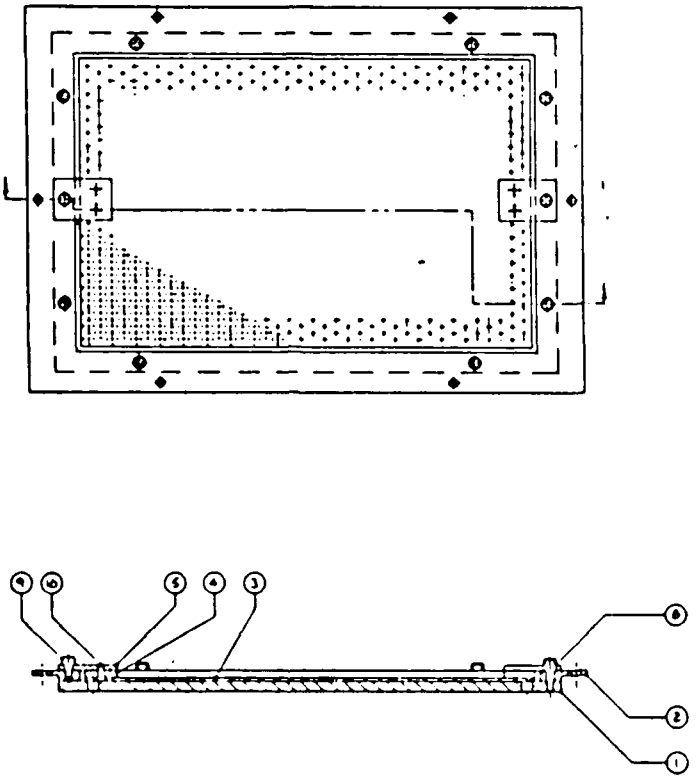

FIGURE 3-23. ROLLER END IMPLANTATION HOLDER.

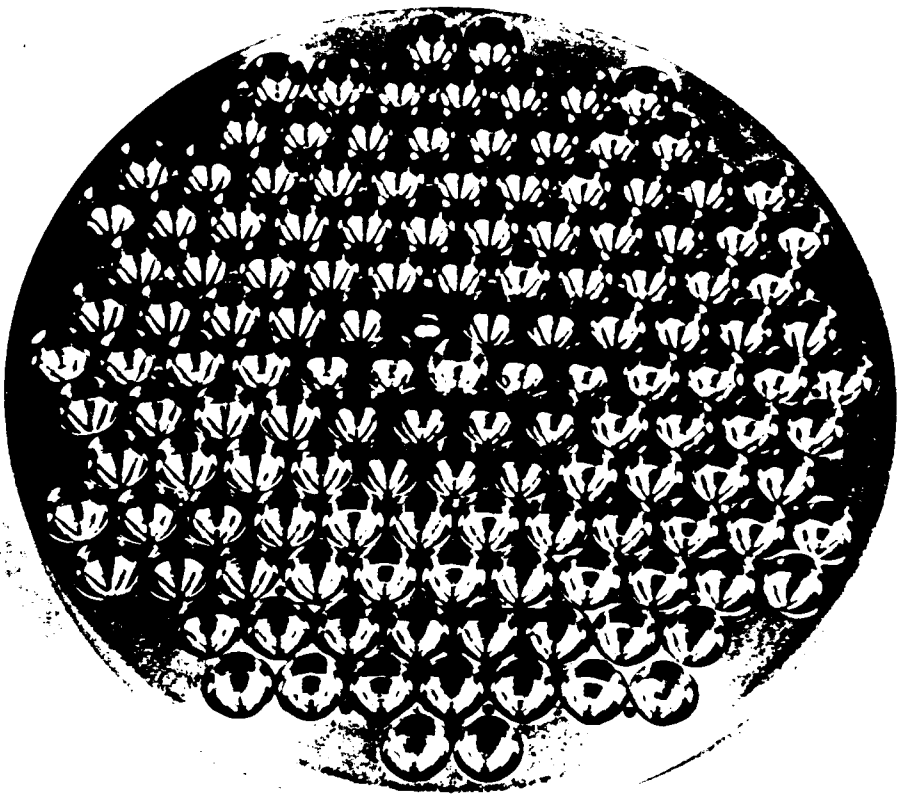

FIGURE 3-24. FIXTURE USED TO IMPLANT M-50 BALLS.

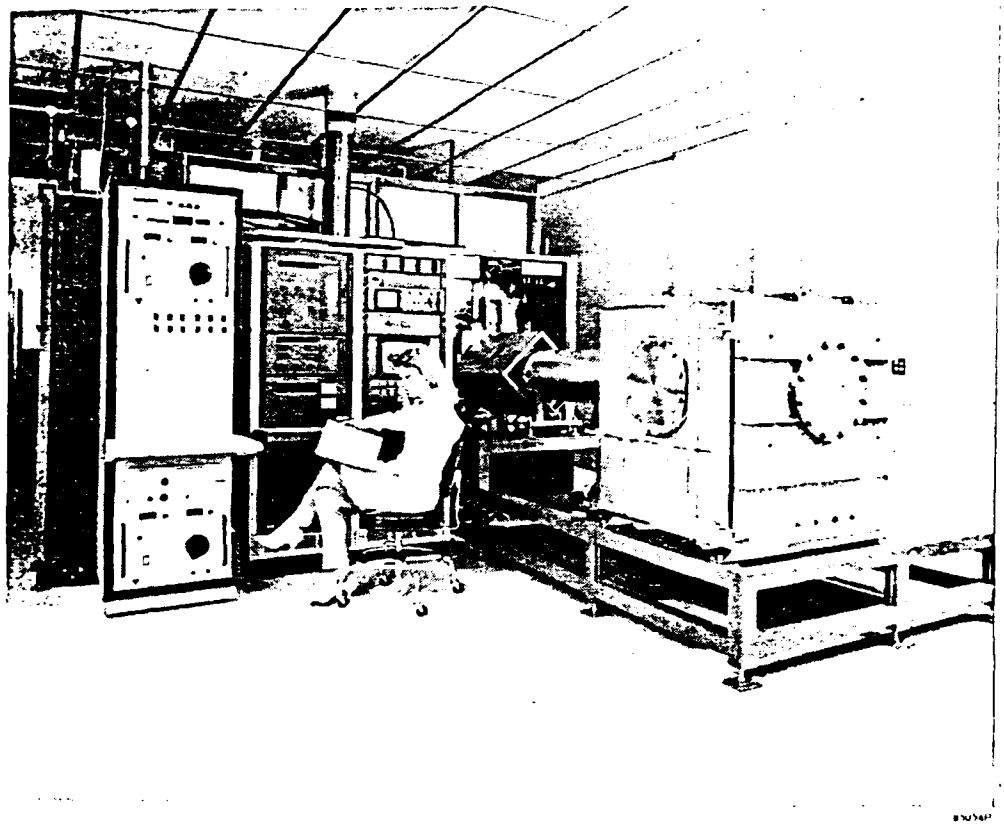

FIGURE 3-25. MANTECH FACILITY AT TIME OF INSTALLATION.

3.3.1 Ion Beams Obtained

Ion beams are obtained in most commercial implanters by creating a plasma (positive ions plus electrons) containing ions of the element of interest in an ion source such as shown in Figures 3-26 and 3-27.

The negatively biased hot filament emits energetic electrons which ionize the atoms in the source, creating a plasma when pressure rises above a critical background value. Normally, elemental species are introduced into the ion source via a gaseous charge or by heating a volatile compound of the species to sufficiently high temperatures so that its vapor pressure will sustain a plasma arc. Positive ions are extracted from the plasma by an electrode and injected into the mass analysis/beam transport system shown in Figure 2-1.

The technique used to produce heavy metal (i.e., Cr^+) ions for the ManTech program utilized a chlorine containing vapor (Cl_2 or Freon) in the ion source. The gas reacts with the chromium side walls of the source to produce chromium chloride, which is subsequently disassociated in the plasma to allow intense metal ion beams to be produced. Table 3-1 lists a number of ions obtained, charge material used, and the beam intensities achieved. A disadvantage of producing metallic ions by this chlorination technique is that considerable deposition of excess metal chlorides occurs in various parts of the beam transport system. This is not normally a problem for the other listed ion beams. Nitrogen has been extracted at the 5 mA level. A test was made with other possible feed gases, but no increase in available mass analyzed current was observed. The limited peak energy of the implanter, 160 keV, prevents the use of N_2^+ for most 100 keV applications.

Figure 3-28 shows a typical mass spectrum obtained for Cr^+ when using the chlorination technique. The source lifetime using the chlorination technique is typically 8-12 hours and represents a limitation on system efficiency due to the need to thoroughly clean the source housing after each source change.

The ion beams were measured by employing Faraday cups with a 0.079 cm^2 circular aperture in a 5 mil Ta sheet positioned in front of a (-200 V) secondary electron suppression electrode which in turn was in front of a shielded, 2 cm long cylindrical (Faraday) cup. These were calibrated using Rutherford Backscattering spectroscopy.

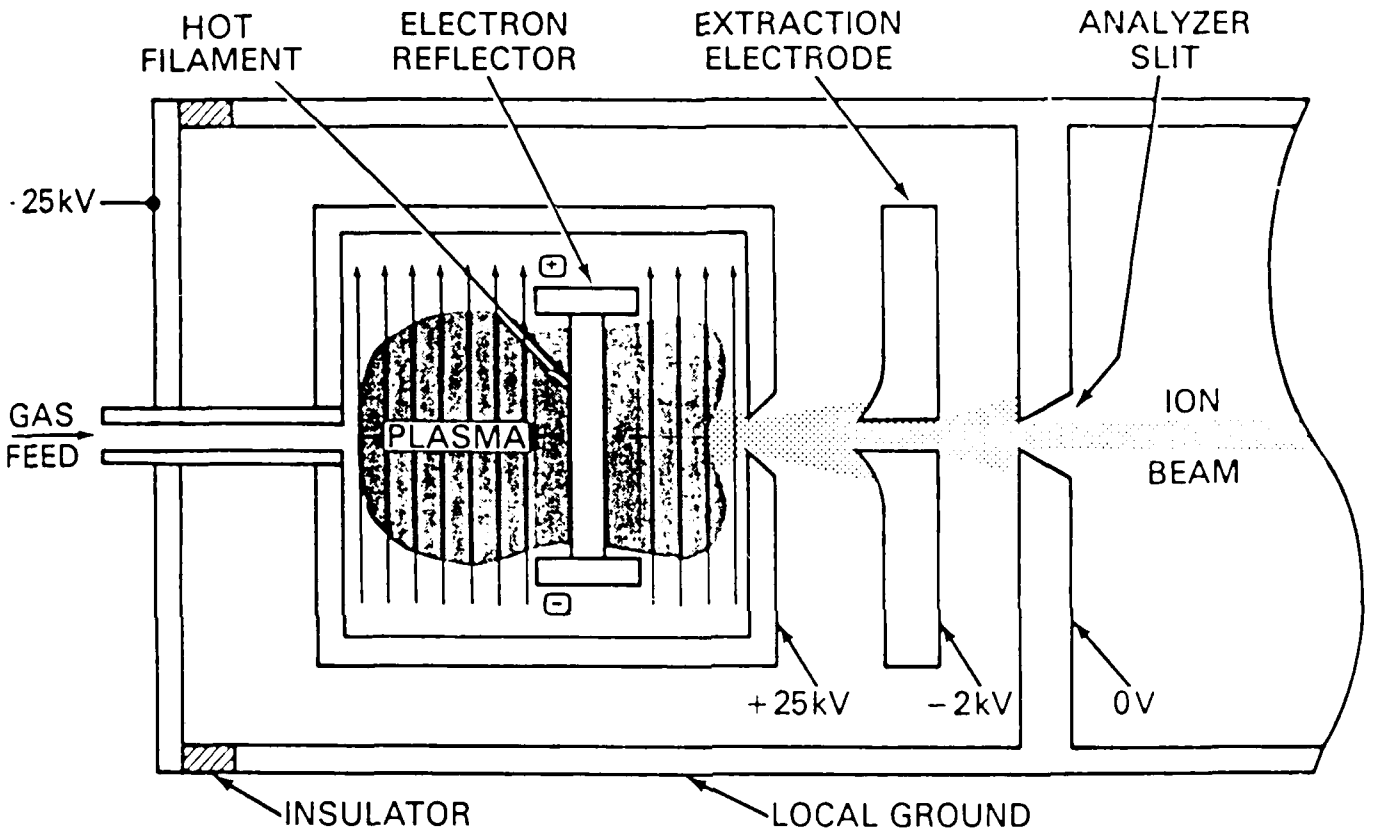

FIGURE 3-26. SCHEMATIC OF ION SOURCE USED IN MANTECH IMPLANTER.

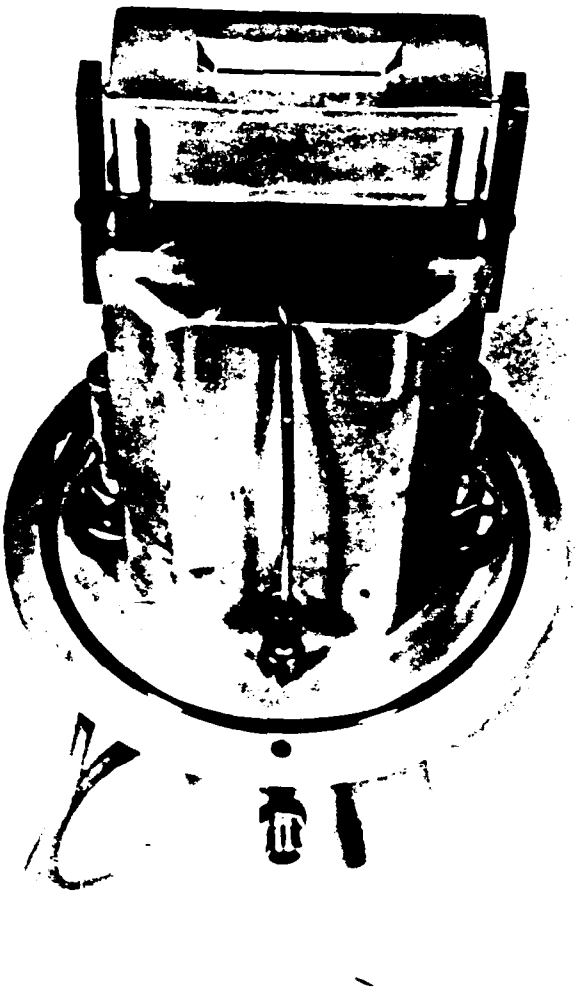

FIGURE 3-27. PHOTOGRAPH OF FREEMAN ION SOURCE.

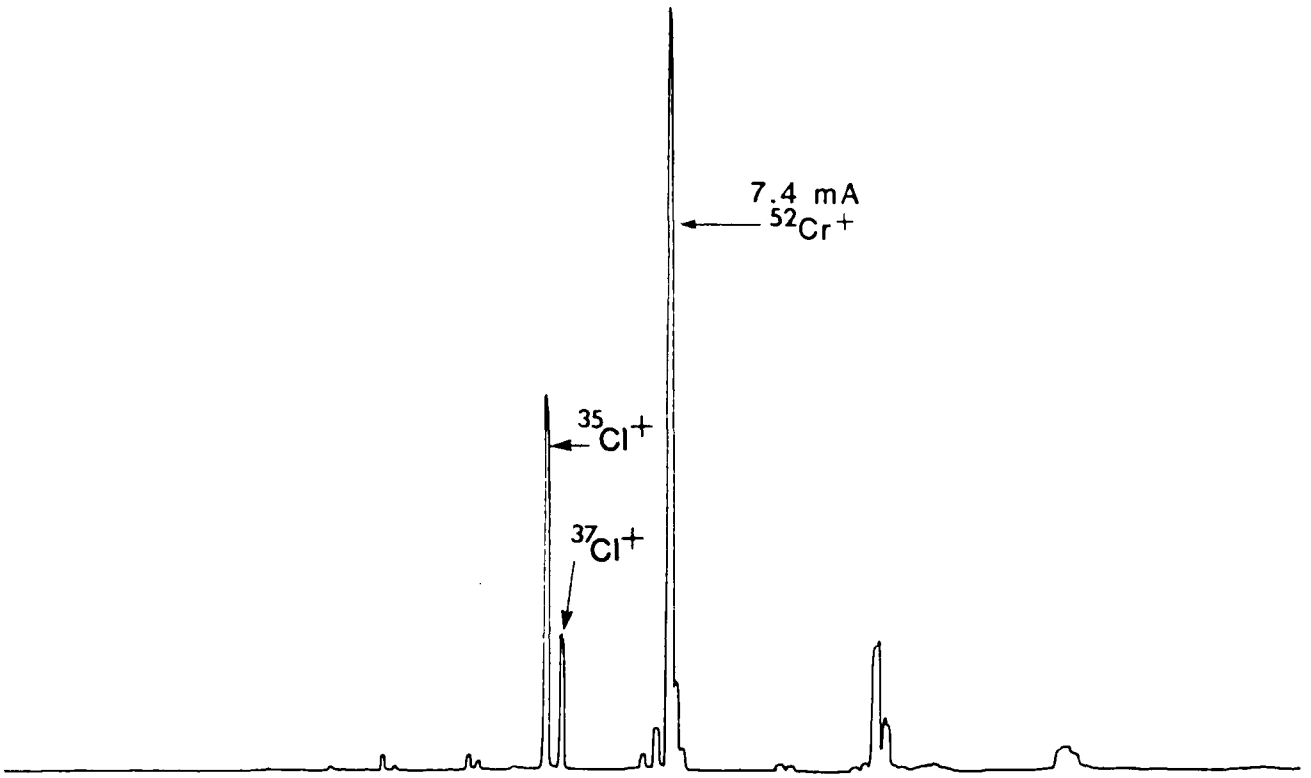

FIGURE 3-28. MASS SPECTRUM SHOWING 7.4 mA ^{52}Cr ION BEAM.

TABLE 3-1. METAL ION BEAMS PRODUCED IN MANTECH IMPLANTER.

Application	Ion Species (Charge)	Ion Current Obtained (Millamperes) Typical	Best
Wear:	Titanium (Cl_2 + Ti)	5	8
	Carbon (50 keV) (C))	5	8
	Nitrogen (N_2) (N^+ @ 50-170 keV/atom)	5	7
	Nitrogen (N_2) (N_2^+ @ 25-85 keV/atom)	10	12
	Molybdenum (Cl_2 + Mo)	3	5
Corrosion:	Chromium (Cl_2 + Cr)	7	13

3.3.2 Ion Implanter Problems

During the initial installation and try out of the implanter, a large number of problems occurred to impede operations. Several of these are listed in Table 3-2. Almost all the causes of machine downtime have since been remedied. Arcing in the high voltage power supply was fixed by replacing the isolation transformer. The chance of damage to circuit components from these high voltage arcs is now reduced.

Ion source and source extraction residue build-up continues to be a problem when running chlorination (i.e., Cr^+). However, the frequency of extraction region cleaning has been reduced by allowing the source arc to extinguish itself with gas turned off. This seems to reduce the amount of condensed residue upon cooling down the source for rebuilding.

Residue build-up is most likely the cause of extraction arcing and suppression overloading. The only remedy to this is frequent disassembly and cleaning of the entire source extraction region. Over the period of operation, this amounts to 2-3 hours of cleaning every 9 shifts (3 days of continuous 3 shift operation).

TABLE 3-2. CAUSES OF IMPLANTER DOWNTIME FOLLOWING INSTALLATION.

Implanter Function	Nature of Problem Experienced
Ion Source-	Ion Source Housing Required Frequent Cleaning Source Magnet Failure Leaks in Regulators Leak Valves for Source Failed Filament Controller Failed
Extraction-	H.V. Arcs at Source Major Repairs to High Voltage Power Supply Controller Needed Replacing Variac Fell Apart Off Calibration
Magnet-	Jumps off Mass Peak Frequent Circuit Breaker Cut Off
Post Acceleration-	Controller Wanders in Jumps Frequent Sparks in Oil Tank, was replaced
Services-	Water Leaks in Boxes, particularly Compressors, Water Control Panel Power Supply Fail for Relays Power Supply Fail for Control Rack
Control Rack-	Vacuum Controller Board Replaced Replaced Master Relay Control Board Replaced AMU Board Replaced Current Readout Board Oscilloscope Channel Replaced
Other-	O-Ring burned in Beam Gate (V3) When System Crashes, Valve Closes w/Beam Optical Links all Replaced Replace Surge Diodes in Post Accel Suppressor and Fuses Frequent Need to Reset Controller for Optical Link at Terminal Faraday Flag Wire Broke Beam Shield in Magnet Not Installed Correctly
End Station-	All Welds in Magnet Drive Leaked H_2O, Contaminated Rough Pump Oil Installed Carbon Mask to Prevent Raster Beam from Hitting Pipe Some Water Leaks in Rotary Drive, Seals were Improved Kinked Hose to Rotary Drive, Replaced

The in-line end station gate value "O-ring" burned occasionally upon machine shutdown, but the frequency of this was reduced by fixing the high voltage arcing problem. A circuit has been installed to prevent this problem from recurring.

The major cause(s) of downtime in the second year of operation involved breakdown of machine components (electronics, etc.) whose normal lifetimes are being approached. In addition, continual use of the chlorination technique places strong pressure on corrosion prone machine components such as vacuum pumps and fittings. Frequent (every other week) cleaning is performed to avoid lengthy downtime.

SECTION 4
TUNGSTEN CARBIDE TOOLING PROJECT

A program was implemented to ion implant cobalt-cemented tungsten carbide tooling with nitrogen ions since many reports of wear improvement of this composite are in the open literature.

4.1 WC-Co PUNCHES

The first phase of this program performed in conjunction with Borg-Warner and Kenametal Corp. was to implant a set of WC-Co punches in Spire's existing implantation facilities so that the improvement in punch lifetime, if any, can be determined.

Two vendors have provided the WC material. These samples differed in the amount of cobalt binder present (6% and 9%) to provide interesting comparison information. Preliminary screening examinations were performed by Borg Warner on all punches to identify possible imperfections which could compromise the test results. SEM analysis as well as precision dimensional measurements were obtained and are described in Spire document PP-10089-01 submitted to NRL in April 1984.

A total of 81 punches were implanted. These represent nine samples each of a variety of parameters including the beam energy, punch material, and punch type. Two punch types are used, a "piercing" punch to make a starting hole and a "shaving" punch to make the precision hole. Worst case hole tolerance is only 0.4 mils, and thus punch lifetime is relatively short. A meeting was held with personnel at Borg-Warner and at their Morse Chain Division and a test procedure formulated to optimize the amount of useful lifetime data obtainable without interfering with critical production schedules.

Figure 4-1 shows the geometry used to carry out the nitrogen implantation. Nitrogen beam energies of 75 and 150 keV were selected with corresponding doses of 4×10^{17} N/cm^2 and 6.5×10^{17} N/cm^2 used.

Preliminary testing of the set of 80 nitrogen-implanted punches was performed at the Morse Chain Division of Borg Warner. The test took place during December 1984. A technical problem was immediately learned by the Spire representative at the test.

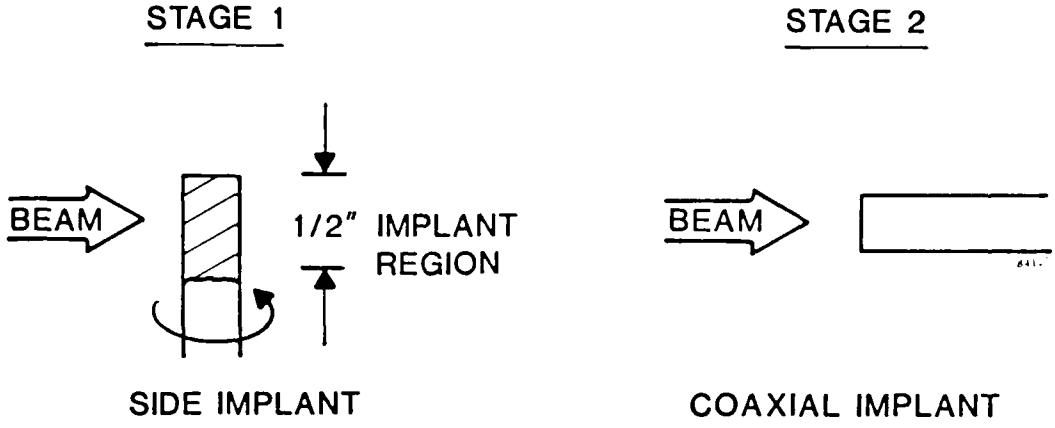

FIGURE 4-1. PILOT PRODUCTION IMPLANT.

The tolerances on the holes punched in the chain are very high, on the order of ten thousandths of an inch. Since it is not practical to machine the punches to this precision and because of variations from one position to another in the multiple punch press, the operator "stones" each punch selectively before initiating full production. A few samples are produced, errors in tolerance identified, and individual punches are ground in place to meet tolerances.

It was obvious that this stoning process would remove the ion implant and it was reluctantly agreed by Morse Chain that a run of out-of-tolerance product would be made to give the implanted punches a fair test. Very preliminary indications are that perhaps a 23% improvement in lifetime has been achieved with the implant, but this value is too small to be a clear, non-statistical benefit. After this run, the production group at Morse Chain declined to waste further output, so all further punches were stoned. As expected, no change in lifetime compared to controls was observed on the second run following this "stoning."

The process of stoning was surprising to both the Spire and Borg Warner representatives at the test. Despite the several earlier meetings, the subject had never been mentioned by the Morse Chain people. It would appear that if these early results continue, this application of ion implantation would be inappropriate for commercial exploitation for these specific types of tooling.

4.2 WC-Co PRINTED CIRCUIT BOARD DRILLS

In addition to WC-Co punches, Spire also investigated nitrogen implantation of cemented tungsten carbide printed circuit board (PCB) drills for improved wear resistance. The program was performed in cooperation with Digital Equipment Corporation, a major computer manufacturing company. A few samples were also sent to L.C.O.A. Technical Center for careful laboratory evaluation in parallel with the field evaluation at Digital.

The process parameters (ion energy, ion dose, possible substitute choice for nitrogen) were identified in accordance with the best available data on the treatment of cemented WC available at the time. (Temperature during implantation will exceed 200°C, etc.). A large batch of PCB drills was obtained from Digital for use throughout this work. The initial focus was on Digital's stainless steel shant carbide drill bits (0.0135 inch and 0.0453 inch diameter) used to drill 250 mil thick boards made from 14 mil cores constructed of type 7628 glass.

100 PCB drills from Digital were implanted with 120 keV N^+ ions to a dose of $2.5 \times 10^7 N/cm^2$, at the geometries shown below (Figure 4-2). This geometry was chosen to minimize sputtering of the Co binder that has been seen previously doing commercial service work. Prior to implantation, the drills were marked on their shank during examination under an optical microscope to ensure that all drills could be aligned equivalently during implantation to achieve the geometry shown in Figure 4-2. Prior to implantation, a thermocouple was attached to a drill tip and was measured to attain 310° C using a 3.9 mA (total) defocused 120 keV N^+ ion beam. The current density at the position of the drills was 42 microamp/cm^2. During implantation the drills were held in a square matrix of holes and tilted slightly so as to expose each shank at least 0.1" from the tip.

The aim was to keep the tip temperature above 200°C to prevent a softening of the WC matrix which has been seen by Harwell researchers at lower temperatures and below 500-600°C where nitrogen out diffusion has been seen by GTE workers. This batch of one hundred drills consisted of fifty (50) 13.5 mil. diam. The PCB drills were sent to Digital for evaluation with a select number being sent to Lamination Corp. of America (L.C.O.A.) for independent evaluation.

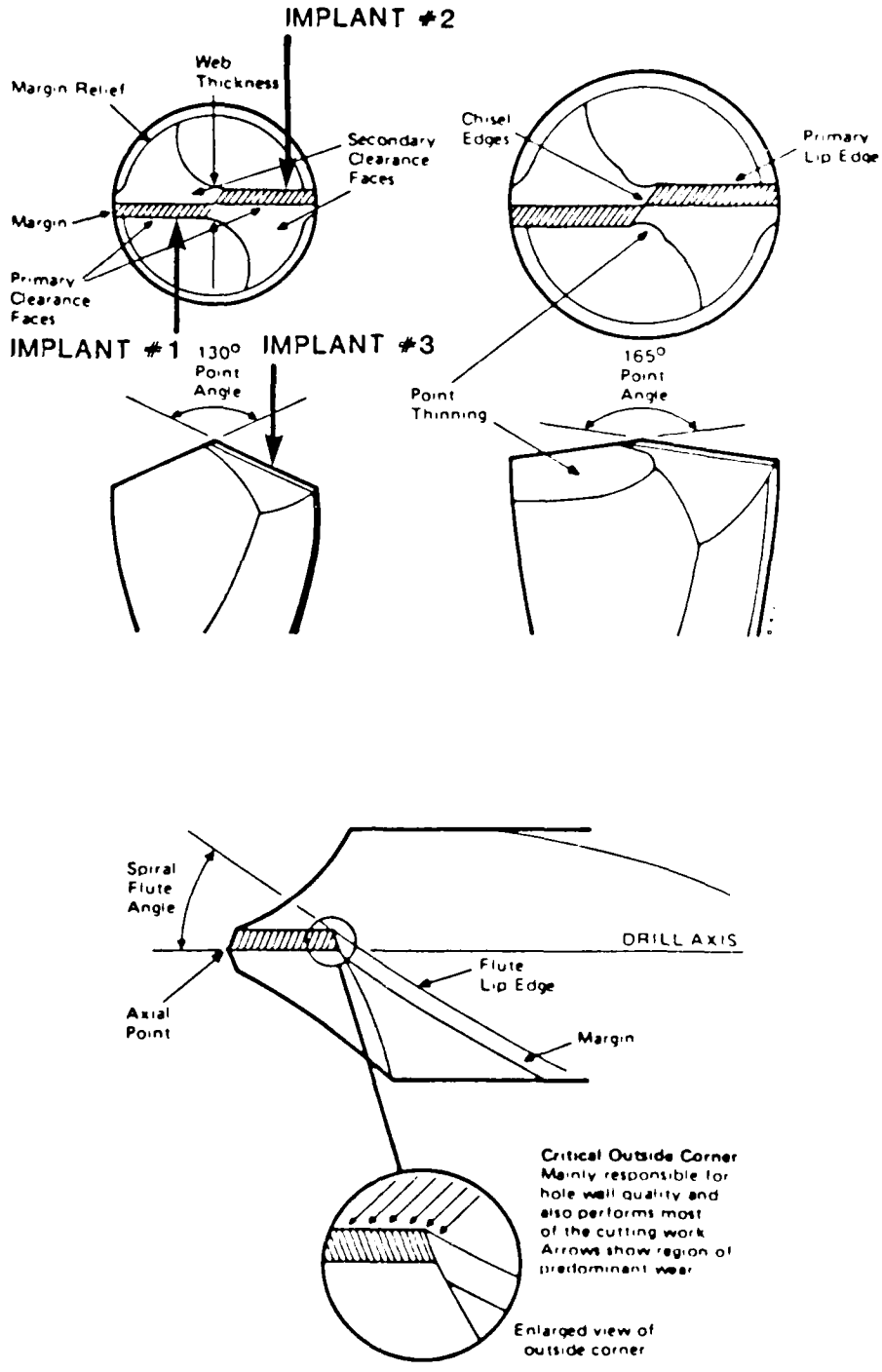

FIGURE 4-2. GEOMETRIES USED FOR PCB IMPLANTATION.

The Digital tests on these first N-implanted drills were sparse and statistically inconclusive with a hint of earlier breakage of N-implanted drills during successive plunge tests into fiberglass boards.

Results of Digital's preliminary PCB "Hit" tests:

1) 45 mil drills - no breakage on either nonimpl. or N-impl. after 4600 hits

2) 13.5 mil drills:

   a) 80K rpm, 43 ipm feed rate
   nonimpl. #1 - 1730 hits before breaking
   nonimpl. #2 - 1930 hits before breaking
   N-impl. #1 - 1140 hits before breaking
   N-impl. #2 - 650 hits before breaking

   b) 80K rpm, 64 ipm feed rate
   nonimpl. #1 - 115 hits before breaking
   nonimpl. #2 - 1580 hits before breaking
   N-impl. #1 - 178 hits before breaking
   N-impl. #2 - 11 hits before breaking

   c) 80K rpm, 80 ipm feed rate
   nonimpl. #1 - 5 hits before breaking
   nonimpl. #2 - 280 hits before breaking
   N-impl. #1 - 210 hits before breaking
   N-impl. #2 - 7 hits before breaking

L.C.O.A. performed SEM evaluation of unimplanted and implanted 45 mil drills.

Following are test results from a drilling study evaluating the performance of ion implanted drills compared to the performance of standard (control) drills with respect to drilling temperatures, drill wear, and burr heights.

The evaluation was performed by L.C.O.A. Technical Center (Project #1-039) for the Spire Corporation.

I - DRILLING CONDITIONS

1. Materials:
   - 3 High stack of 0.059" double-sided 1/1 FR-4
   - 0.093" Foilboard Backup
   - 0.014" Entry Overlay Plus
   - Spire supplied solid carbide, relieved #57
   - Standard (control) and ion implanted drills

2. Parameters:
   - 600 SFM surface speed
   - 3 Mil/Rev chip load
   - 53,300 RPM
   - 160 IPM infeed rate
   - 1,000 IPM retraction rate
   - 60 PSIG pressure foot pressure
   - 0.040" penetration into backup
   - 0.500" height above stack (drill tip)
   - 4,000 hits (12,000 holes)

TABLE 4-1. BURR HEIGHTS (MILS).

	CONTROL DRILLS			ION IMPLANTED DRILLS		
	Test 1	Test 3	Test 5	Test 2	Test 4	Test 6
Entry Burr						
Panel 1	0.4	0.3	0.4	0.3	0.5	0.3
Panel 2	0.4	0.4	0.3	0.4	0.4	0.4
Panel 3	0.3	0.3	0.2	0.4	0.4	0.4
Exit Burr						
Panel 1	0.4	0.3	0.3	0.3	0.3	0.3
Panel 2	0.3	0.3	0.2	0.4	0.3	0.3
Panel 3	0.4	0.3	0.2	0.2	0.4	0.3

TABLE 4-2. AVERAGE BURR HEIGHTS (MILS).

	Control	Ion Implant
Entry Burr		
Panel 1	0.33	0.37
Panel 2	0.37	0.40
Panel 3	0.27	0.40
Exit Burr		
Panel 1	0.33	0.30
Panel 2	0.23	0.33
Panel 3	0.30	0.30

TABLE 4-3. DRILLING TEMPERATURES (°F).

	CONTROL DRILLS			ION IMPLANTED DRILLS		
Number of Hits	Test 1	Test 3	Test 5	Test 2	Test 4	Test 6
Start	403	396	373	387	385	388
500	421	422	416	406	415	413
1,000	439	453	439	418	442	436
1,500	450	469	456	435	455	454
2,000	462	482	470	452	464	463
2,500	468	492	478	463	469	474
3,000	476	499	486	474	475	482
3,500	491	505	492	482	482	491
4,000	502	511	493	489	487	498

TABLE 4-4. AVERAGE DRILLING TEMPERATURES (°F).

Number of Hits	Control	Ion Implant
Start	391	387
500	420	411
1,000	444	432
1,500	458	448
2,000	471	460
2,500	479	469
3,000	487	477
3,500	496	485
4,000	502	491

TABLE 4-5. DRILL WEAR (MILS).

	CONTROL DRILLS			ION IMPLANTED DRILLS		
	Test 1	Test 3	Test 5	Test 2	Test 4	Test 6
Land wear	0.49	0.56	0.39	0.52	0.56	0.70
Rounding	0.46	0.17	0.34	0.34	0.60	0.27
Total Wear	0.95	0.73	0.73	0.86	1.16	0.97

TABLE 4-6. AVERAGE DRILL WEAR (MILS).

	Land Wear	Rounding	Total Wear
Control	0.48	0.32	0.80
Ion Implanted	0.59	0.40	0.99

Their report concludes that no significant differences were found when comparing the ion implanted drills to the control drills in the areas investigated. An average drilling temperature difference of approximately 10°F was noted, with the control drills producing the higher temperature. Because of the temperature variations larger than 10°F from drill to drill within the groups, the average temperature difference is not significant.

The average wear exhibited by the ion implanted drills is 0.2 mil higher than that of the drills in the control group. Since drill wear varies more than 0.2 mil within the groups, the average wear difference may be normal for these particular drills and not attributable to ion implantation. The difference between the average burr heights is negligible considering that irregularities in laminates and stacking procedures alone can cause variations of such magnitudes.

For these reasons, the second set of drills was implanted with Ti using the same geometry as in Figure 4-2. The rationale for choosing Ti was to encourage the formation of intermetallics to strengthen the Co binder phase. As in the case of N-implantation, no noticeable performance benefits were observed in drilling tests (Digital) or in L.C.O.A. analysis.

4.3 RECOMMENDATIONS ON WC-Co TOOLING

It is apparent from the results of these tests that the effects of nitrogen implantation on WC-Co is still very poorly characterized compared to other applications in tool steels or titanium alloys where positive results are routinely found.

Part of the problem arises from testing in an industrial environment (i.e., the "stoning" on the Borg-Warner test punches) and part may come from the Co content and grain size of the WC composite. Spire personnel have seen some applications of fine grain (submicron) grade WC-Co where nitrogen implantation actually appears to weaken the matrix leading to premature tool wear. Because of the present uncertainties regarding successes versus failure for nitrogen implanted WC-Co tooling, Spire is not actively pursuing these applications until the classes and grades of WC-Co helped by nitrogen implantation are better identified. It should be noted that there are very few laboratory wear tests in the open literature on N-implanted WC-Co as compared to tool steels. Substrate temperature, grain size, and Co content and alternative implant species would appear to be the main parameters for further studies.

SECTION 5
OPERATION OF FACILITY

The following sections describe the operating experience gained in implanting the different bearing components for the Man Tech program. Since all M50 alloy bearing components were received (and sent back) in an oil preservative it was necessary to thoroughly clean them prior to implantation. The following cleaning procedure was adopted after consultation with NRL (B. Sartwell) and NARF-North Island (G. Kuhlman) personnel.

5.1 CLEANING PROCEDURE

TABLE 5-1. NRL BEARINGS - CLEANING PROCEDURE.

1. Remove bearing component from shipping bag. Find serial number on component, if applicable. Mark a new ziplock bag with the serial number and put the other bearing parts (e.g., inner race, rollers and roller retainer) still in the original bag, inside the new bag.

2. Wipe oil off races with Kay-dry tissues then wipe with tissues dampened with paint thinner (napthalene).

3. Ultrasonically clean bearing components in napthalene, 5 mins; acetone, 5 mins; and finally, methanol, 5 mins.

4. Change methanol if excessive spotting is seen on dry bearings.

5. After methanol cleaning go over each component and wipe with Kay-Dry tissue dampened with methanol. Removal all spots, inside and outside. Pay especially close attention to sharp corners or ridges cleaning roller ridges with Q-tip and methanol.

6. Mount components on platter, taking them from cart kept under laminator air flow. Blow races off with nitrogen before mounting on platter. Mount with S/N side down.

5.2 BEARING PROCESS EXPERIENCE

Initially it was planned for Spire to design and build implantation fixtures to treat 100 each of the M50 alloy bearings listed below:

1. H-46 Hinge Pin Bearings
2. Helicopter Gear Box Bearings
3. J-79 Main Shaft Engine Bearings
4. T-58 Bearings
5. T-64 Bearings

Problems were experienced at NARF-North Island in releasing T-64 and T-58 bearings from inventory, so 200 additional H-46 bearings were implanted instead.

5.2.1 Implantation of H-46 Hinge Pin Bearings

Using the fixture design shown in Figure 5-1, the inner races of two hundred H-46 hinge pin bearings were implanted with 150 keV Cr to a fluence of 2×10^{17} Cr/cm^2. During the trial runs it was found that it was necessary to use compressive spring washers under the expansion screws to exert an elastic force on the copper D-holders to compensate for the outward thermal expansion of the races on the D-holders caused by beam heating. The inner race dimensions are: I.D. = 3.10 inches, O.D. = 3.31 inches, width = 2.10 inches.

For treatment, initially two races were mounted end-to-end on the cooling fixture and approximately 0.75 inch of one end of each race was implanted while rotating behind an aperture in a tantalum mask. A movable Faraday cup was located just above the 1.5-inch x 1.5-inch aperture opening and was used to monitor the dose. The surface temperature of the race was measured for 150 keV, 4 mA incident beam. The use of an intermediate soft Al foil as well as installing stiff spring washers kept the temperature rise well within acceptable limits as shown in Figure 5-2.

These implantation took approximately 1.0-1.5 hours beam time per run with a total beam current of 4-5 mA on the implanter Faraday with a current density of about 60 micro A/cm^2 at the target plane. The source was run with chromium sidewalls and freon support gas for internal chlorination. It was found that the buildup of a graphitic-like scale on the inside of the source would cause intermittent breakdown of the arc and resultant source instability requiring source replacement every eight hours or so.

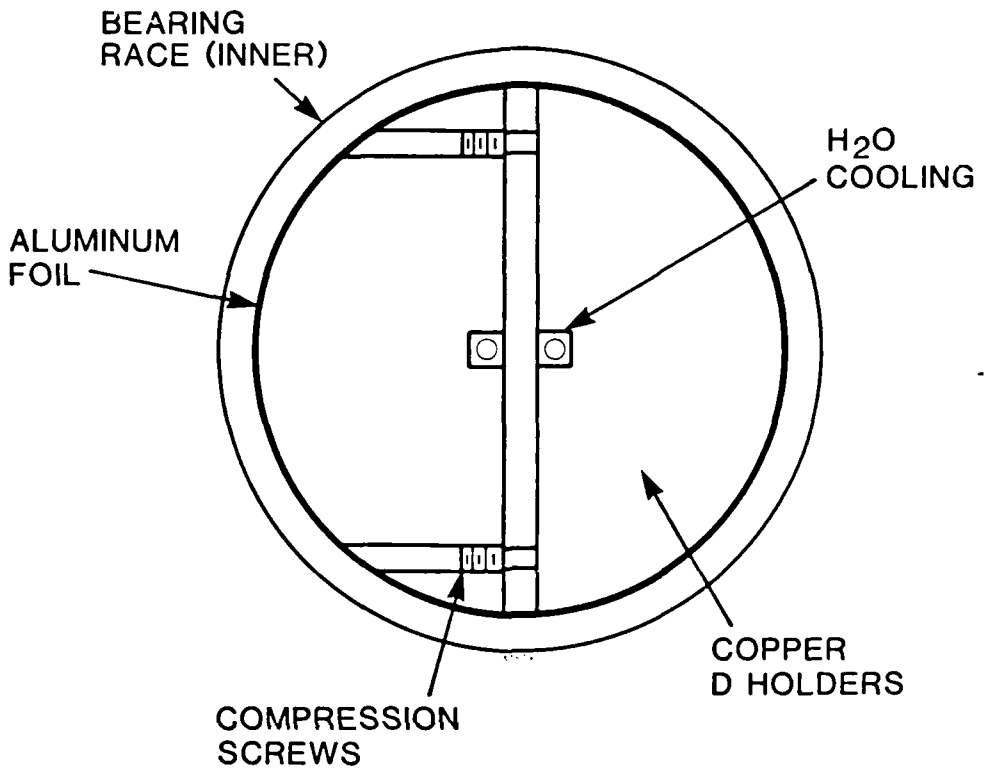

FIGURE 5-1. COOLED FIXTURE FOR H-46 INNER RACES (END VIEW).

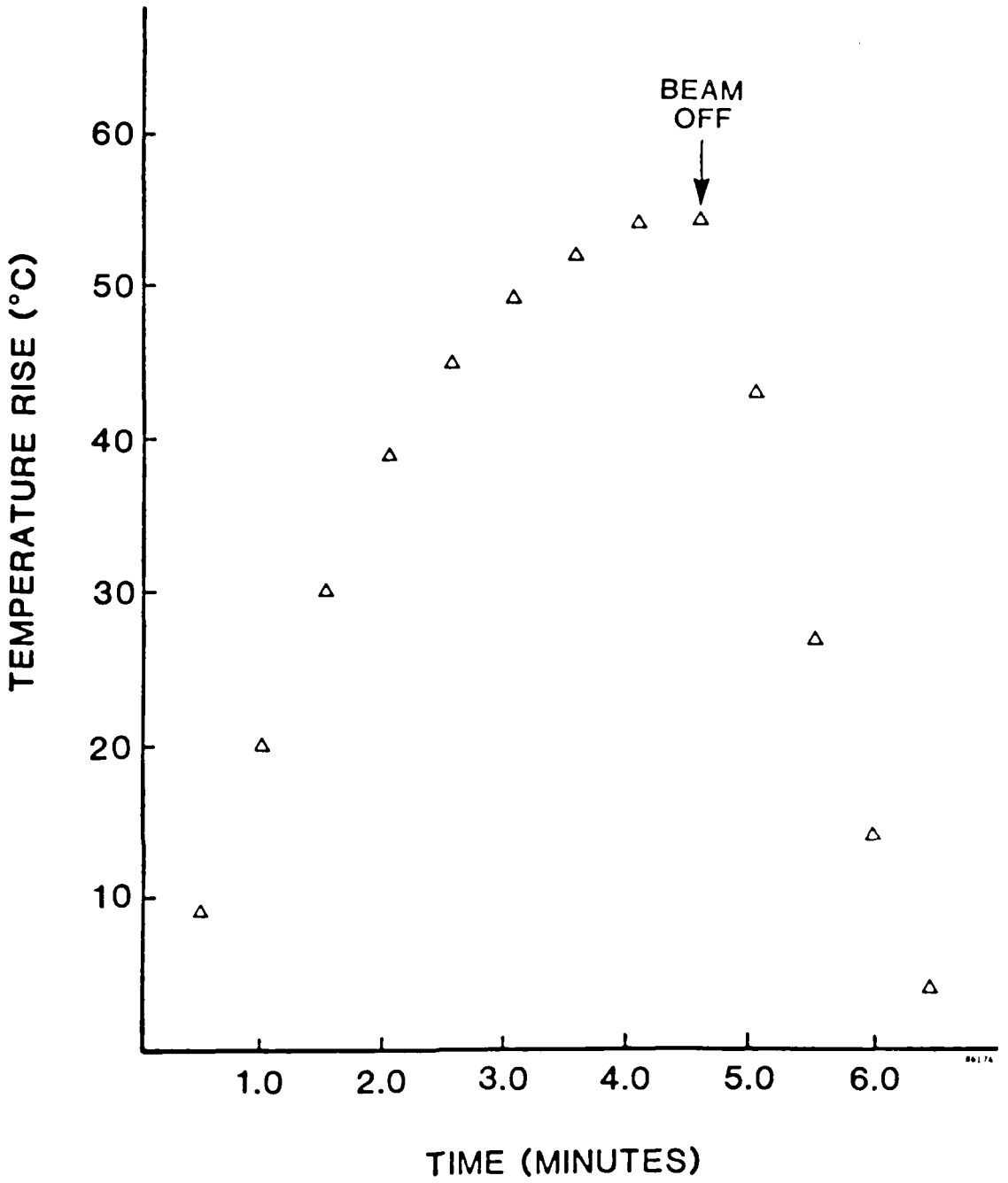

FIGURE 5-2. TEMPERATURE RISE OF H-46 BEARING SURFACE MOUNTED ON COOLED FIXTURE AFTER EXPOSURE TO 150 keV, 4 mA BEAM.

In addition, it is usually difficult to start up a source that has been shut down from operation due to internal sparking, presumably from deposition of volatile chlorides after cooldown. For this reason, 3 shift/day runs were used to implant a majority of the H-46 races. Table 5-2 shows the record of a 12 day run (3 shifts/day) indicating individual run times and required source changes.

The fixture originally designed for this race held 4 races. Another fixture of the same basic design (Figure 5-3) was later constructed to accommodate eight races. However, problems were encountered in maintaining a firm outward force on all races simultaneously so practical operation was limited to six races in a batch. As typical for all new fixture designs, initial trials typically consumed one to two shifts to install and mount bearing components. After such a shakedown trial, subsequent component mounting times for the H-46 inner races were typically 20-40 minutes as shown in Table 5-2. Other typical process times are given in Table 5-3.

5.2.2 HELICOPTER GEARBOX BEARING

This bearing had a complement of fourteen (14) rollers and an inner and outer race to be implanted using the fixtures described in Section 3.2.3. The water cooled fixture allowed implantation of 18 outer races per batch, Figures 5-4 and 5-5. The mask assembly shown in Figure 5-5 was used to i) reduce the thermal load on the bearing and, ii) restrict the angle of incidence the implant makes with the race surface to within $\pm$ 30° from the normal. The outer race dimensions are: I.D. = 2.125 inches, O.D. = 2.250 inches, width = 0.50 inches.

The fixture used to implant the inner races (Figure 3-17) was based on the design shown in Figures 5-1 and allowed closer packing and therefore better utilization of the beam. This fixture utilized a tantalum mask in front of the races to limit the beam to $\pm$ 30° from normal to the surface. The inner race dimensions are: I.D. = 1.175 inches, O.D. = 1.440 inches, width = 0.525 inches.

In both cases, a Faraday cup was used to monitor and integrate the Cr beam. In the case of the outer races, it was placed in a corner of the rectangular beam scan used to implant the elliptical array presented by the tilted circular platen holding the races. For the case of the inner races, the Faraday cup was positioned beyond the horizontal rotating array and the beam was overscanned to cover the Faraday cup. Tables 5-4 and 5-5 give the processing tiomes for the various components of the helicopter gear box bearings.

TABLE 5-2. H-46 RACE PROCESSING AND TARGET CHANGE TIMES.

DATE	RUN NO.	BEAM TIME (HRS.)	CHANGE TIME	COMMENTS
1986				
1/10	3	1:30		Source Change
	4	2:20	--	
1/13	5	1:30	--	
1/13	6	1:10	--	
1/13	7	1:30	:35	Source shorts, rebuild
1/13	8	1:18	:30	
1/14	9	1:40	--	Clean Arc Chamber
1/14	10	1:40	:30	
1/14	11	1:40	:30	Lost Hi-Vac
1/14	12	1:20		
1/14	13	1:30		
1/14	14	2:00	--	Source Change
1/14	15	1:20	:30	C Buildup
1/14	16	1:00		Change Source (1425 hr) on source-on meter
1/15	17	1:00		
1/15	18	1:10		
1/15	19	0:50	:20	
1/15	20	1:14	:40	
1/15	21	1:10		New Source (1439 hr)
1/16	22	2:00		
1/16	23	1:13		
1/16	24	1:00	:25	
1/16	25	0:50		
1/17	26	--		
1/17	27	1:05		
1/17	28	1:00	:60	
1/17	29	1:05		New Source (1469 hr)
1/17	30	1:00	:25	
1/17	31	0:45		
1/17	32	1:08	:20	

TABLE 5-2. H-46 RACE PROCESSING AND TARGET CHANGE TIMES (Continued).

DATE	RUN NO.	BEAM TIME (HRS.)	CHANGE TIME	COMMENTS
1986 1/17	33	1:05	:45	
1/21	34	0:55		Optional Source Change (1476 hr)
1/21	35	1:00		
1/21	36	1:00		
1/21	37	1:05	:30	
1/21	38	1:15	:40	Optional Source Change (1468 hr)
1/21	39	1:00	:20	
1/22	40	1:05		
1/22	41	0:55		
1/22	42	0:50		
1/22	43	--		
1/22	44	1:00		
1/22	45	1:00		
1/22	46	0:50	0:35	
1/22	47	0:50	0:25	
1/22	48	1:10	0:35	
1/23	49	1:05		New Source (1506 hr)
1/23	50	1:00	0:20	
1/23	51	1:20		
1/23	52	0:40		
1/23	53	0:50		Opt. Source (1512 hr)
1/23	54	1:05		
1/23	55	1:03	0:23	
1/23	56	1:00		
1/23	57	--		Rebuild Source (1521 hr)
1/24	58	0:50		
1/24	59	0:50	0:25	
1/24	60	0:55	0:35	
1/24	61	1:01	0:50	Opt. Source (1526 hr)

TABLE 5-2. H-46 RACE PROCESSING AND TARGET CHANGE TIMES (Concluded).

DATE	RUN NO.	BEAM TIME (HRS.)	CHANGE TIME	COMMENTS
1986				
1/24	62	0:55		
1/24	63	0:45	0:35	
1/24	64	1:00		
1/24	65	0:55		
1/24	66	0:55		
1/24	67	1:00		New Source (1537 hr)
1/24	68	0:50		
1/24	69	1:30		
1/24	70	0:30		Opt. Source (1541 hr)
1/25	71	0:50		
1/25	72	0:45	0:20	
1/25	73	0:35	0:30	
1/25	74	0:50	0:25	
1/25	75	0:50	0:20	
1/25	76	0:40	--	
1/25	77	0;45	0:30	New Source (1552 hr)
1/25	78	0:50		
1/25	79	0:50	0:25	
1/25	80	1:00	0:50	
1/25	81	--		
1/25	82	0:50		
1/26	83	0:50		
1/26	84	0:40		
1/26	85	0:50	0:25	
1/26	86	0:45	0:25	New Source (1566 hr)
1/26	87	0:40		
1/26	88	1:00		
1/26	89	0:55		
1/26	90			Power Supply Problems Stop Runs

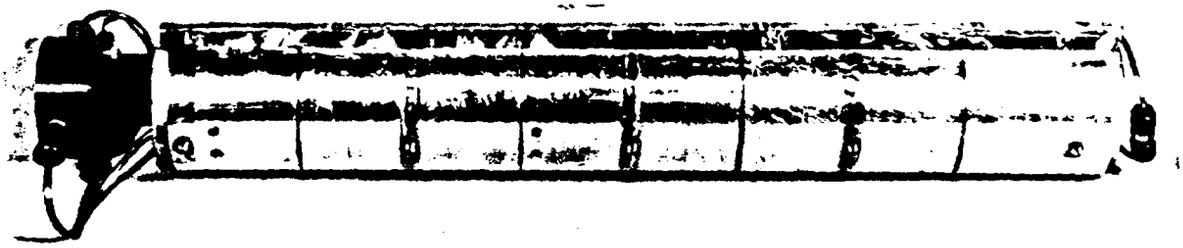

FIGURE 5-3. FIXTURE FOR IMPLANTING H-46 INNER RACES.

TABLE 5-3. PROCESSING TIMES FOR H-46 BEARINGS.

Cleaning time (6-8 races):	1/2 hour
Mounting on fixtures:	1/4 hour
Positioning fixture in chamber:	1/4 hour
Pump down time (to 3×10^{-6}):	1/2 hour
Beam setup time:	3/4 hour (per batch)
Beam time: per pair (beam moved vertically to scan different pairs of bearing races)	1 hour

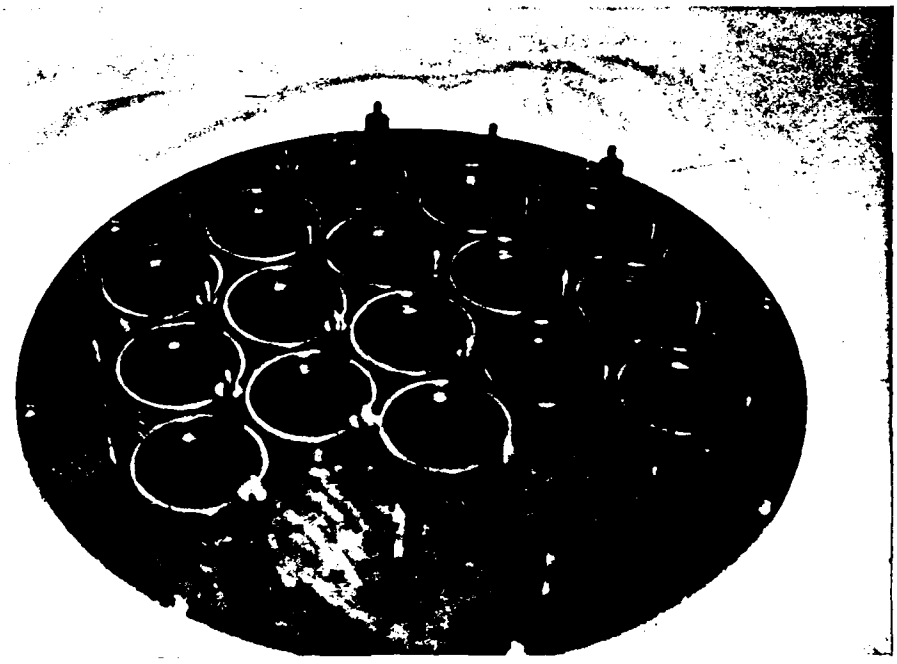

FIGURE 5-4. BASE PLATE OF IMPLANTATION FIXTURE FOR OUTER RACES OF HELICOPTER GEAR BOX BEARINGS.

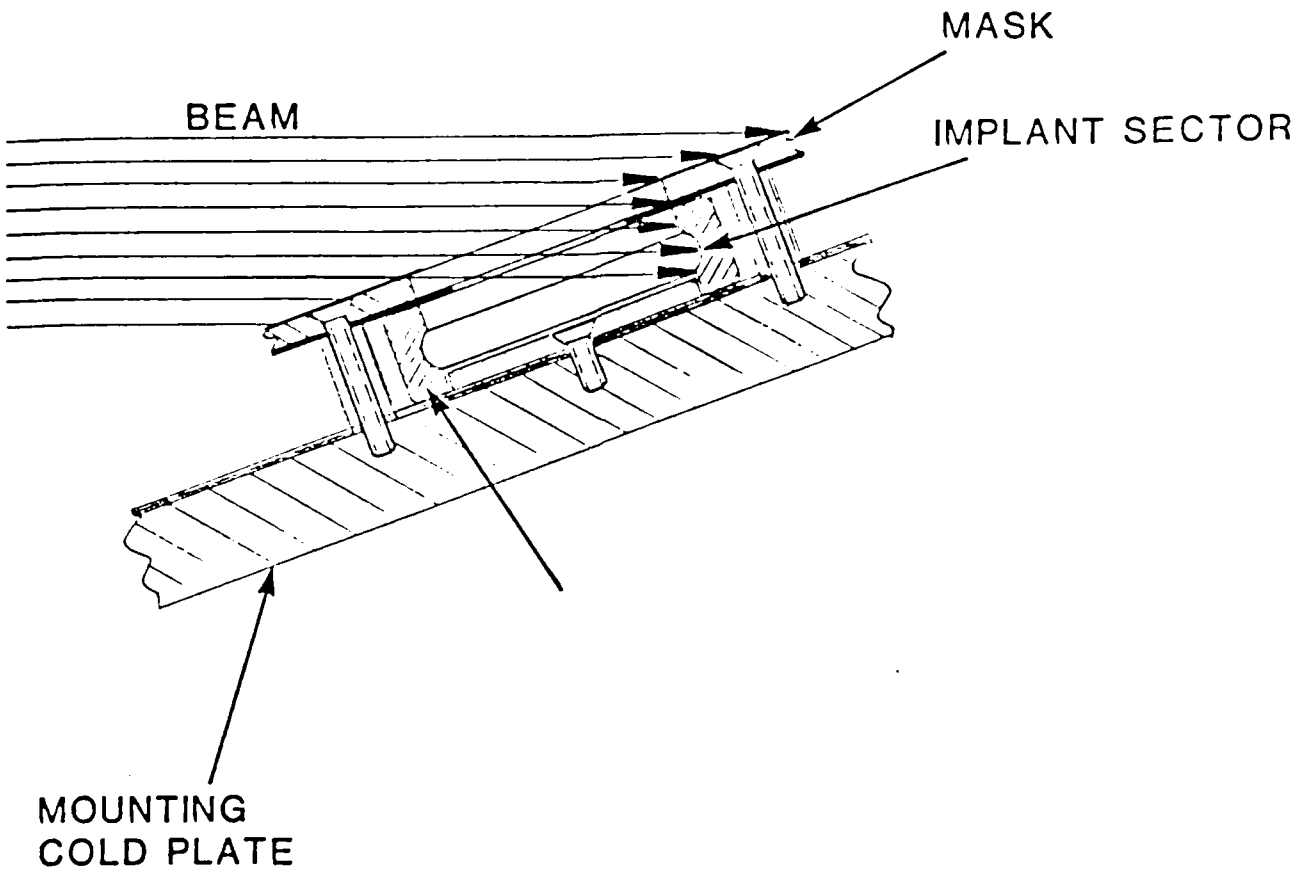

FIGURE 5-5. OUTER RACE FIXTURING.

TABLE 5-4. PROCESSING TIMES FOR HELICOPTER GEAR BOX RACES.

	Outer Races (18/Batch)	Inner Races (12/Batch)
Cleaning times:	1 1/2 hours	1 hour
Mounting on fixture:	1 hour	1 1/4 hours
Positioning fixture in Chamber:	1/4 hour	1/4 hour
Pumpdown time (to 3E-6 torr):	1/2 hour	1/2 hour
Beam setup time:	1/2 hour	1/2 hour
Beam times:	4 1/2 hours	4 1/2 hours

The gearbox bearing rollers (0.25-inch long x 0.25-inch diameter) required implantation of both ends as well as the circumference. The ends were done by holding the rollers in a stainless steel plate honeycomb drilled with holes (14 x 38 matrix) for support. Initially the rollers were to be held to a water cooled plate by a magnetic field but this approach was not used for the roller ends and radiation cooling was used to keep the rollers below 250°C (Figure 5-6). This limited the beam current to about 3 mA. This method was time consuming from the viewpoint of loading and unloading and keeping the various rollers from individual bearings segregated during cleaning, loading, processing, and unloading.

TABLE 5-5. PROCESSING TIMES FOR HELICOPTER GEAR BOX ROLLERS (ENDS) 38 BEARINGS/BATCH (14 rollers per beaming.)

Cleaning:	10 hours
Mounting in Fixture:	2 hours
Positioning Fixture:	1/2 hour
Pumpdown time:	1/2 hour
Beam setup time:	1/2 hour
Beam time:	1 1/2 hour per end

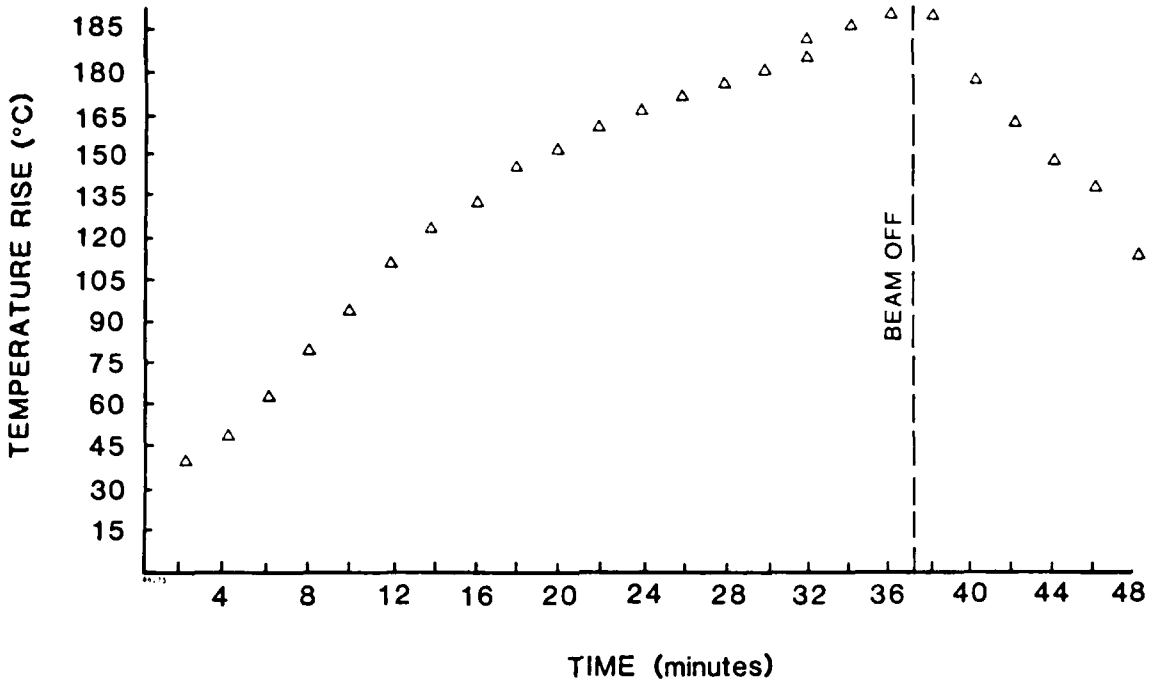

FIGURE 5-6. TEMPERATURE RISE OF GEAR BOX OUTER RACE AS A FUNCTION OF TIME AT 120 keV BEAM, 3 mA.

The circumferential areas of the roller were implanted in a fixture (Figure 5-7) which held 18 rows of bearing rollers. Rotation of the rollers was initially planned using a magnetic hold-down device shown in Figure 3-20 but was later changed to using a multiple (alternating field) magnet plate. The rotation of the rollers was to be achieved by frictional rolling of the rollers in their fixture against a moving water cooled stainless steel plate located between the rollers and multi-magnet array. Small (5°) movements of the rollers were obtained by rotating a 1/4-20 threaded shaft coupled to the roller assembly. This motion was controlled by the machine operator at regular intervals throughout the implant period. Each incremental motion was designed to rotate the rollers by 5° with 60 movements per implantation to ensure uniformity. Ta masks placed in front of the rollers limited the implant angle to within $\pm$ 30° of the normal.

Four runs of rollers were carried out and the following problems were encountered.

1. Although the magnetic holdown fixture worked well in air, several rollers were observed to become stuck during the first implantation. This was thought due to tight tolerances and metal-to-metal welding of the sputter cleaned bearing surface to the fixture. Those rollers showing evidence of uneven rolling were reimplanted.

2. A post implantation examination by NRL showed a fall off of Cr dose on some of the outermost rollers due presumably to an underscanning of the beam.

3. An interior water cooling line burst during processing of the fourth batch causing total machine shutdown with no obvious damage to rollers.

Table 5-6 lists the processing times associated with the sides of the helicopter gear box bearings.

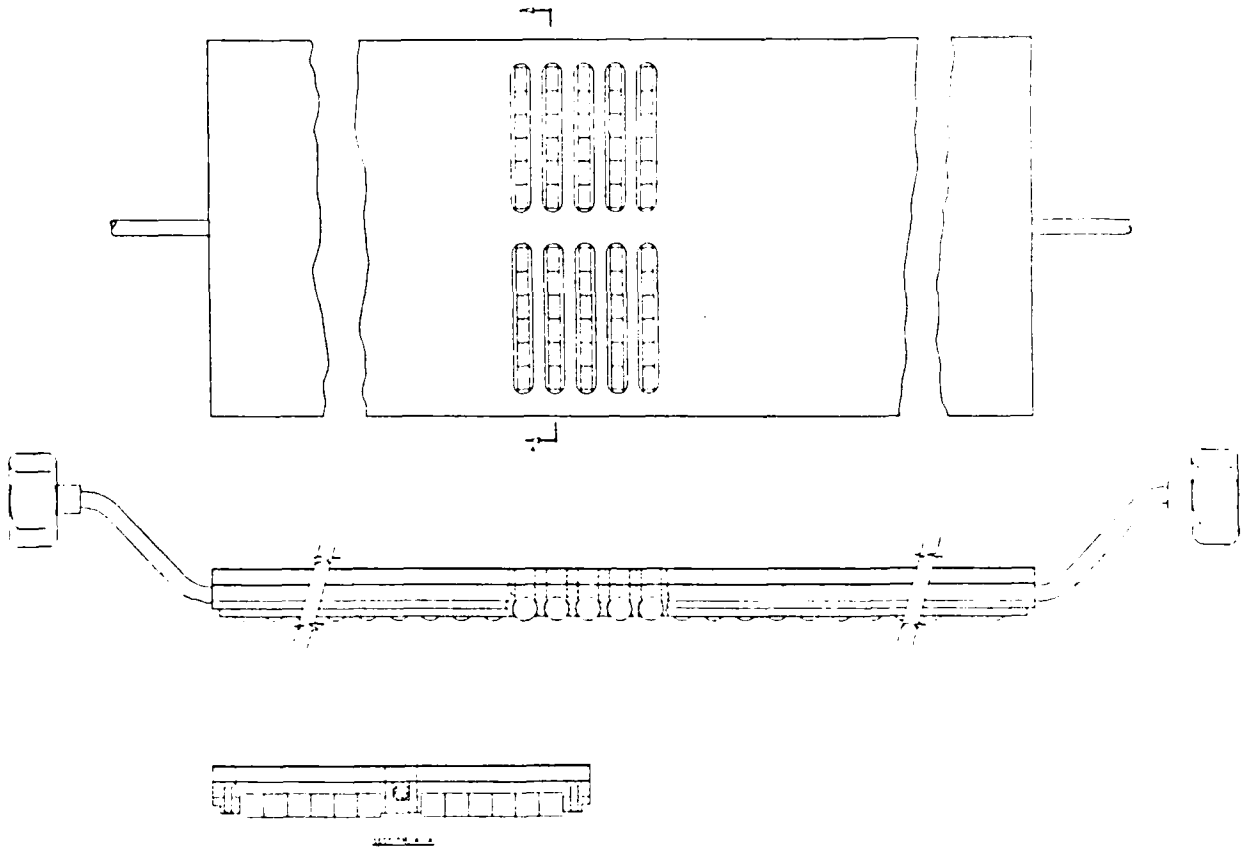

FIGURE 5-7. ROLLER FIXTURE.

TABLE 5-6. PROCESSING TIMES FOR HELICOPTER GEAR BEARINGS (SIDES) 18 BEARINGS/BATCH (14 rolls per bearing).

Cleaning:	4 hours
Mounting in Fixture:	2 hours
Positioning Fixture:	1/2 hour
Pumpdown Time:	1/2 hour
Beam Setup Time:	1/2 hour
Beam Time:	4 1/2 hours

5.2.3 J-79 Bearing - Balls, Inner and Outer Races

The fixtures for implanting the (split) inner races of the J-79 bearings consist of water cooled copper plates which are sandwiched between the split rings under compression for cooling. The fixture holds ten split rings at a loading. The inner rings have a 6.0-inch I.D., a 7.0-inch O.D. and are about 0.5-inch wide each. The outer race has a 8.75-inch O.D., a 7.75-inch I.D. and a width of about 1.5 inches.

The initial design for the outer race fixture also employed stainless steel annular rings to be placed between the (5) races during implantation for cooling and shielding. Besides cooling, they were supposed to shadow the upper half of the race surface beneath it which is at a highly oblique angle to the beam and thereby prevent undue sputtering from that surface. Unfortunately, the shield itself sputters and subsequently deposits s.s. onto the shielded portion of the race above it.

Consequently, we were forced to change to an implantation geometry whereby we could do a single implant at a shallow angle to the race surface. Figure 5-8 shows a water cooled rotating fixture used to implant J-79 outer races, three at a time. The rather large spacing between the races is required to avoid shadowing, but significantly reduces the beam utilization efficiency. A much more efficient method would be to implant one race at a time (minimal beam sweep) with i) adequate thermal clamping and ii) a fast sample changing mechanism with no break in the vacuum. Unfortunately, we were not able to redesign and build such a fixture so late in the program.

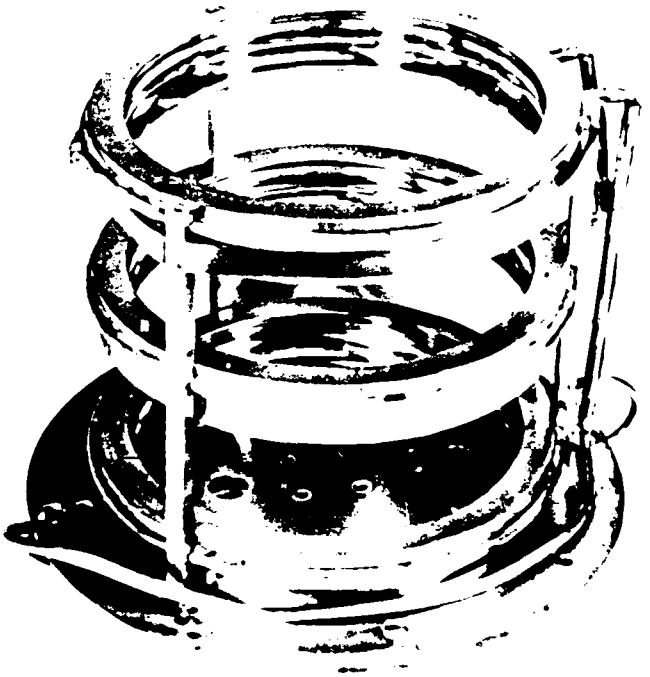

FIGURE 5-8. WATER COOLED FIXTURE FOR J-79 OUTER RACES.

TABLE 5-7. PROCESSING TIMES FOR J-79 RACES.

	SPLIT INNER (10 per batch)	OUTER (3 per batch)
Cleaning:	1 hour	1 hour
Mounting:	2 hours (initial) 1/2 hour thereafter	2 hours (initial time)
Positioning:	1/2 hour	1 hour (initially)
Pumpdown time:	1/2 hour	1/2 hour
Beam setup:	1/2 hour	1/2 hour
Beam time:	5 1/2 hours	1 1/2 hours

J-79 balls (0.875-inch diameter) were processed in the fixture shown in Figure 3-24. After loading this fixture with balls, an overlying stainless steel mask with matching hole positions was used to constrain the balls in the hole pockets as well as physically restrict the beam to hitting the central portion of the balls. The fixture was attached to a wafer cooled platen (Figure 3-16) by means of a small angle (5°) wedge to cause forward and backward motion of the balls as well as sidewise rolling during rotation of the fixture during implantation. The implantation times were dictated by the maximum temperature rise allowed (250°C maximum ball temperature) as measured on a sample ball with a thermocouple. Table 5-8 gives the pertinent processing times for the J-79 balls.

TABLE 5-8. PROCESSING TIMES FOR J-79 BALLS (120 PER BATCH MAXIMUM)

Cleaning:	4 hours
Mounting:	3/4 hour
Positioning:	1/2 hour
Pumpdown time:	1/2 hour
Beam Setup:	1/2 hour
Beam time:	16 1/2 hours

5.3 STAFFING REQUIREMENTS FOR FACILITY

The highest efficiencies on the NRL Man Tech facility are obtained when operated at a full 3 shifts/day. This is of course largely due to the fact that no time is lost in startup and cool-down procedures. If the machine operators have shifts which overlap by at least 1/2 hour then there is adequate time for the transfer of critical information and the processing is completed as desired. The shifts presently employed are 7:30 a.m. to 4:00 p.m., 3:30 p.m. to 12:00 a.m., and 11:30 p.m. to 8:00 a.m., and appears to work very well. The qualifications generally sought for this level of technician is an associates' degree (or equivalent work experience) in electronics or mechanical engineering with a background in electromechanical devices. Previous experience with ion implantation is helpful but not necessary due to the fact that the NRL Man Tech facility's end station and ion optics are so different from typical semiconductor type operations.

A facility supervisor is also extremely important to provide an interface to technical staff personnel. The role of the supervisor is to organize the work to be done, translate technical specifications into machine parameters, ensure proper inventory levels, and act as the "machine expert" solving problems beyond the capabilities of the operators. The supervisor should have a Bachelor of Science degree in electronics or mechanical engineering with a strong physics background.

SECTION 6
COST ANALYSIS OF FACILITY OPERATION

6.1 BEARING PROCESSING COSTS

The costs associated with implanting bearing components must take into account the hourly rate for implanter time and the time to process a batch. Each of these depends on a number of other factors. Table 6-1 gives an hourly rate cost breakdown based on 1, 2, or 3 shift operation. Projected processing costs for a dedicated facility will be based on the three shift operation since this is the principal mode of operation in which the Man Tech implanter has been used.

Figure 6-1 shows the percent utilization of the Man Tech implanter since the start of its operation. The hatched sections of the histogram represent maintenance time while the remainder includes Man Tech time, development time, and commercial service work. It can be seen that its utilization corresponds to and sometimes exceeds a 5 day week, 3 shifts a day level after an initial startup period of several months. As expected, the efficiency of treating individual components increases with experience, and this is reflected in lower processing costs.

Processing costs scale with the following parameters:

1. Dose: 2×10^{17} Cr/cm^2 at 120 keV for all M50 bearing components
2. Area: The total area beam must cover.
3. Geometrical factor: A number by which the dose must be multiplied to account for beam only hitting a fraction of component at one time
4. No. of implants: Number of individual implantations required because of geometry restrictions or need to spread out distribution in depth
5. Ion beam current: Process time scales inversely with available beam current subject to beam heating limitations.
6. Reload and pumpdown times: Time to remove one batch and replace with another and time to pump down from atmospheric pressure to acceptable implantation pressure to begin (i.e., 3×10^{-6} torr)
7. Packing density: The line-of-sight limitation of ion implantation, the geometry of the component, and the design of the fixture determines the limiting total size which must be implanted to treat the area of interest.

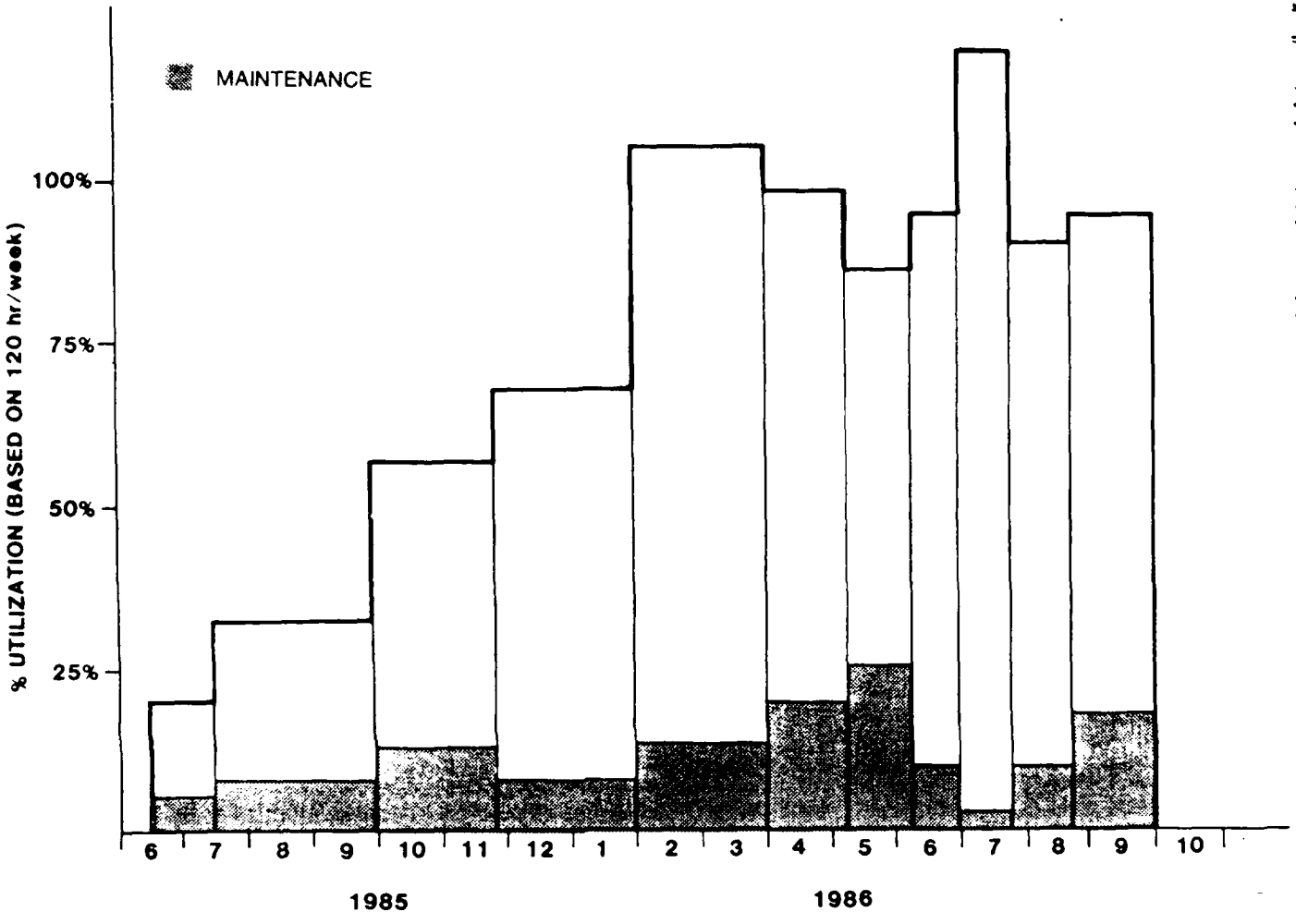

FIGURE 6-1. UTILIZATION OF MAN TECH IMPLANTER FROM 6/85 TO 10/86.

TABLE 6-1. CALCULATION OF HOURLY RATES FOR DEDICATED IMPLANTER FACILITY.

	1 SHIFT	2 SHIFTS	3 SHIFTS
ASSUMPTIONS:			
CAPITAL INVESTMENT	1000 K	1000 K	1000 K
YEARS AMORTIZED	10	10	10
WORK YEAR (HOURS)	2000	4000	6000
AVAILABILITY (PER CENT)	83	85	87
REVENUE HOURS	1660	3400	5220
COSTS:			
CAPITAL EQUIPMENT	100 K	100 K	100 K
LABOR + OVERHEAD + G & A	100 K	159 K	219 K
MATERIALS + G & A	14 K	22 K	25 K
FACILITIES, MAINTENANCE + G&A	27 K	41 K	48 K
TOTAL ANNUAL COST:	241 K	322 K	392 K
HOURLY RATE:	145 $	95 $	75 $

The factors are included in the expression at the top of Table 6-2 which allows calculation of batch hours for particular components which leads to the associated costs in the right hand columns.

Table 6-2 gives actual experience data drawn from the fall-winter 1985 tri-strip, in which the initial setup time is explicitly included. Table 6-3 taken from mid-term operation shows considerably lower costs due mainly to reduced setup times. These costs were for components already processed on the machine as well as projected times (for costs) for bearings not yet received from the Navy.

Table 6-4 gives projected costs for a dedicated future facility based on the same design of fixtures used in the present program.

TABLE 6-2. BEARING IMPLANTATION PROCESSING COST ANALYSIS - ACTUAL EXPERIENCE.

$$\text{BATCH HOURS} = \frac{1.6E\ 19 * \text{DOSE} * \text{GEOM. FACTOR} * \text{AREA} * \#\ \text{OF IMPLANTS}}{.005\ \text{AMPERES} * 3600\ \text{SECONDS}} + \frac{\text{SETUP HOURS}}{\#\ \text{OF BATCHES}} + \text{RELOAD HOURS}$$

BEARING TYPE	DOSE x10E17	GEOM. FACTOR	AREA SQ. IN.	# OF IMPLANTS	BATCH SIZE	RELOAD HOURS	(1) SETUP HOURS	# OF BATCHES	BATCH HOURS	HOURS/ PART	COST/PART @ $ 90/HR	COST/ ASSEMBLY
146 HINGEPIN BEARING												
INNER RACE	2	6	20	1	2	0.5	1.3	100	3.18	1.5882	142.94	142.94
HEL. GEARBOX BEARING												
OUTER RACE	2	5	100	1	18	0.5	12	6	18.23	1.0130	91.17	328.26
INNER RACE	2	6	60	2	12	1	10	9	19.26	1.6048	144.44	
ROLLER FLATS (14)	2	1	90	2	532	1	10	8	13.06	0.0246	2.21	
ROLLER ROUND (14)	2	6	72	1	336	1.5	10	5	16.45	0.0490	4.41	

NOTES

(1) SETUP TIME = AVERAGE OF SETUP TIME + IMPLANTER MAINTENANCE + REWORK TIME
(2) NON-OPTIMUM BATCH SIZE
(3) THRUST PADS ARE SET UP FIRST. MAJOR SETUP TIME INCLUDED HERE.
(4) CURRENT = 0.002 AMPERES

TABLE 6-3. BEARING IMPLANTATION PROCESSING COST ANALYSIS - MID-TERM OPERATIONS.

$$\text{BATCH HOURS} = \frac{1.6E\text{-}19 * \text{DOSE} * \text{GEOM. FACTOR} * \text{AREA} * \#\text{ OF IMPLANTS}}{.005\text{ AMPERES} * 3600\text{ SECONDS}} + \text{RELOAD TIME}$$

BEARING TYPE	DOSE x10E17	GEOM. FACTOR	AREA SQ. IN.	# OF IMPLANTS	BATCH SIZE	RELOAD HOURS	BATCH HOURS	HOURS/ PART	COST/PART @ $100/HR	COST/ ASSEMBLY
66 HINGEPIN BEARING										
INNER RACE	2	6	16	1	2	0.5	1.60	0.8005	80.05	80
LL GEARBOX BEARING										
OUTER RACE	2	6	105	1	18	0.75	7.98	0.4431	44.31	116
INNER RACE	2	6	28	2	12	0.75	4.60	0.3836	38.36	
ROLLER FLATS (14)	2	1	90	2	532	1	3.06	0.0058	0.58	
ROLLER ROUND (14)	2	6	72	1	336	1	5.95	0.0177	1.77	
64 #0 ROLLER BEARING										
OUTER RACE	2	6	105	2	10	1.5	15.95	1.5952	159.52	257
INNER RACE	2	6	28	1	7	0.5	2.43	0.3467	34.67	
ROLLER FLATS (22)	2	1	48	2	196	1	2.10	0.0107	1.07	
ROLLER ROUND (22)	2	6	72	1	336	1	5.95	0.0177	1.77	
68 #2 BALL BEARING										
OUTER RACE	2	6	105	1	10	0.75	7.98	0.7976	79.76	288
INNER RACE	2	6	28	1	7	0.5	2.43	0.3467	34.67	
BALLS (11)	2	16	100	1	121	0.75	19.10	0.1579	15.79	
71 #2 BALL BEARING										
OUTER RACE	2	6	70	1	5	0.5	5.32	1.0634	106.34	1100
INNER RACE	2	6	49.5	1	5	0.5	3.91	0.7813	78.13	
BALLS (23)	2	16	100	1	48	0.75	19.10	0.3979	39.79	

1| NON-OPTIMUM BATCH SIZE
2| CURRENT = .002 AMPERES

TABLE 6-4. BEARING IMPLANTATION PROCESSING COST ANALYSIS - DEDICATED FACILITY.

BEARING IMPLANTATION PROCESSING COST ANALYSIS

FUTURE FACILITIES 10-Jun-87

$$\text{BATCH HOURS} = \frac{1.6E\text{-}19 * \text{DOSE} * \text{GEOM. FACTOR} * \text{AREA} * \#\text{ OF IMPLANTS}}{.007 \text{ AMPERES} * 3600 \text{ SECONDS}} + \text{RELOAD TIME}$$

BEARING TYPE	DOSE x10E17	GEOM. FACTOR	AREA SQ. IN.	# OF IMPLANTS	BATCH SIZE	RELOAD HOURS	BATCH HOURS	HOURS/ PART	COST/PART @ $ 75/HR	COST/ ASSEMBLY
#46 HINGEPIN BEARING										
INNER RACE	2	4	40	1	8	0.5	1.81	0.2264	16.98	16.98
HEL. GEARBOX BEARING										
OUTER RACE	2	4	80	1	19	0.5	3.12	0.1643	12.32	31.40
INNER RACE	2	4	60	2	48	0.5	3.78	0.0787	5.90	
ROLLER FLATS (14)	2	1	84	2	588	1	2.38	0.0040	0.30	
ROLLER ROUND (14)	2	4	72	1	336	0.5	2.86	0.0085	0.64	
T64 #3 ROLLER BEARING										
OUTER RACE	2	4	75	2	14	1	5.92	0.4225	31.69	59.08
INNER RACE	2	4	50	1	24	0.5	2.14	0.0891	6.68	
ROLLER FLATS (22)	2	1	84	2	588	1	2.38	0.0040	0.30	
ROLLER ROUND (22)	2	4	72	1	336	0.5	2.86	0.0085	0.64	
T68 #2 BALL BEARING										
OUTER RACE	2	4	75	1	10	0.5	2.96	0.2958	22.18	74.33
INNER RACE	2	4	50	1	20	0.5	2.14	0.1069	8.02	
BALLS (11)	2	9	81	1	121	0.5	6.47	0.0535	4.01	
J79 #2 BALL BEARING										
OUTER RACE	2	4	25	1	1	0.05	0.87	0.8693	65.19	245.70
INNER RACE	2	4	60	1	10	0.5	2.47	0.2466	18.50	
BALLS (23)	2	9	169	1	138	0.5	12.96	0.0939	7.04	

[1] NON-OPTIMUM BATCH SIZE
[2] CURRENT = .002 AMPERES

6.2 END STATION COSTS

Total acquisition cost of the end station amounts to $637,698. This is comprised of $80,000 of internal labor, $121,959 of outside engineering services, $184,770 of materials, $114,877 of overhead, and $135,192 of general and administrative expenses. If this end station were to be duplicated today, a reduction in labor costs would be incurred due to the nonrecurring engineering charges on the prototype unit. However, the material charges will in all probability increase due to inflation.

SECTION 7
ADDITIONAL APPLICATIONS

The existence of the Man Tech Implantation Facility has provided for the first time an industrial implantation facility featuring mass analyzed beams. This allows potential industrial users of ion implantation technology a means of evaluating the process on their particular component for the first time without any severe limitations on size. The majority of successful applications of ion implantation for improved surface properties involve either improved wear and corrosion resistance of precision components.

As a direct result of the Man Tech briefing held in May 1986, a large number of DoD suppliers and users of critical bearings have initiated trials to solve wear or corrosion properties. Bearings appear particularly attractive to treatment by ion implantation because: i) there is no dimensional change, ii) low temperature processing is possible and iii) bearing performance and processing costs can be competitive with other treatments (CVD, etc.) and large numbers of components (balls) can be treated per batch. The duplex Ti plus C ion treatment originally studied at NRL has been used for the majority of these trials.

The successful treatment of bearings for the NASA Space Shuttle liquid oxygen pumps is an outstanding accomplishment in the progress of ion implantation technology for aerospace applications. In this application the bearings operate in a hostile (LO_2) environment under high loads and speeds without the possibility of using either conventional or solid lubricants. Implantation appears to be the only surface treatment that alleviates the wear problem of these bearings and is presently being done on a routine basis. Another routine application is the duplex (Ti plus C) implantation of critical cryogenic compressor components where conventional lubricants also can't be used.

In the nonaerospace area, treatment of Ti alloy medical prostheses has already reached a production status with one major company and is on the verge of doing so with anotner company. Spire is currently involved in treating several thousand surgical prostheses in the current year (1987). Zirconium electrodes in the chemical industry also are being routinely processed for wear resistance.

Other precision tools benefitting from implantation include spinerettes for extruding fiberglass and precision holes in jet ink printers for copying machines.

In addition to the ManTech program and the commercial service work, the facility has been extensivewly used in support of other government sponsored research activities, including Small Business Innovative Research Contracts. Over a dozen such contracts have been conducted over the past two years of operation of the facility. A notable example of such a program involves the use of high energy, high dose oxygen implantation to produce a buried oxide layer in silicon for improving the radiation resistance and lowering the power requirements of devices. The NRL ManTech facility enabled most of the commercial wafer suppliers to test and develop this emerging technology for critical DoD applications.

Additional applications will continue to grow as the result of i) increased implantation capability, ii) continued exposure in trade publications, iii) successful trial implantations, and iv) tireless marketing efforts.

END

DATE

FILMED

DTIC

4/88